iScience

CellPress
OPEN ACCESS

Article

The implication of integrative multiple RNA modification-based subtypes in gastric cancer immunotherapy and prognosis

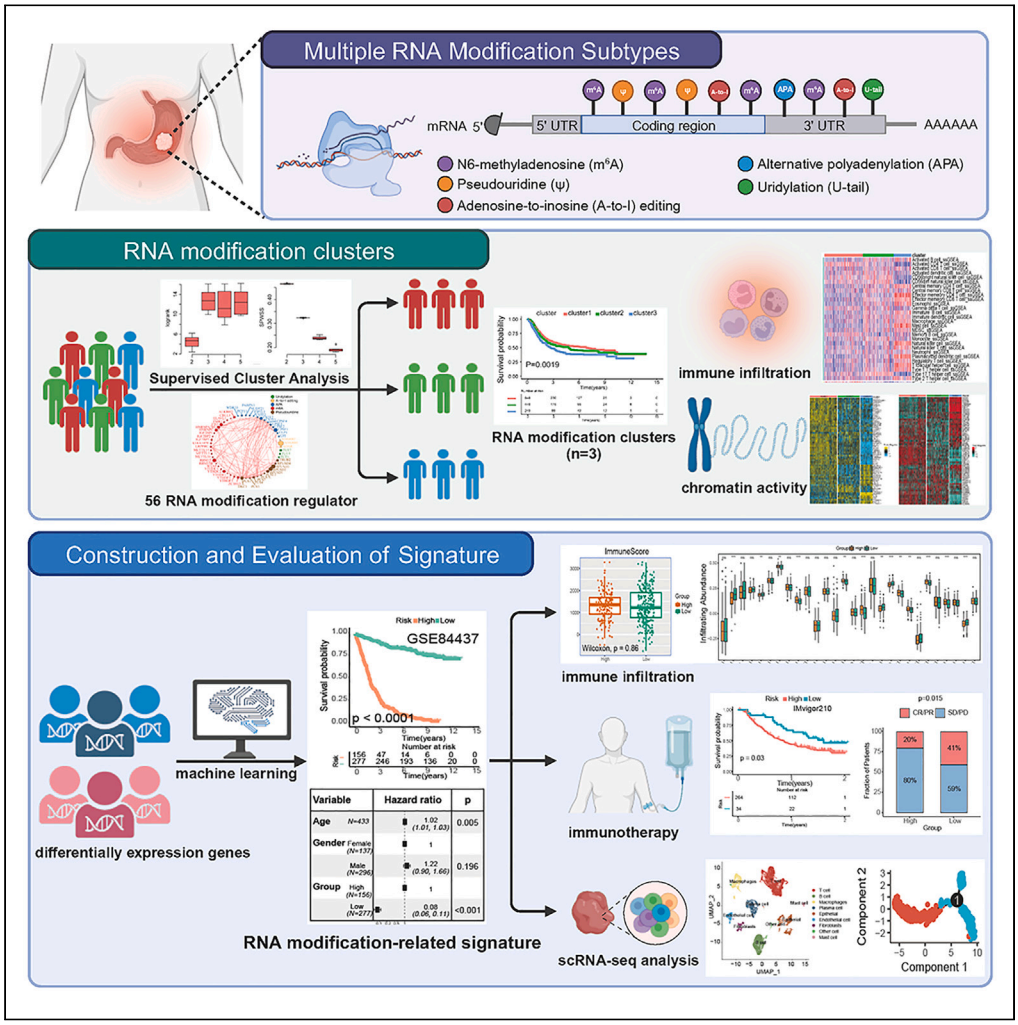

Xiangnan Zhang, Liuxing Wu, Liqing Jia, ..., Lian Li, Kexin Chen, Ben Liu

benliu100@tmu.edu.cn

Highlights

Multiple RNA modification types were comprehensively analyzed

We used machine learning algorithms for screening DEGs in model construction

RNA modification-related signature is a prognostic biomarker for gastric cancer

The identified signature offers the potential to assess the immunotherapy efficacy

Zhang et al., iScience 27, 108897
February 16, 2024
https://doi.org/10.1016/j.isci.2024.108897

iScience

CellPress
OPEN ACCESS

Article

The implication of integrative multiple RNA modification-based subtypes in gastric cancer immunotherapy and prognosis

Xiangnan Zhang,[1,3] Liuxing Wu,[1,2,3] Liqing Jia,[1,3] Xin Hu,[1] Yanxin Yao,[1] Huahuan Liu,[1] Junfu Ma,[1] Wei Wang,[1] Lian Li,[1] Kexin Chen,[1] and Ben Liu[1,4,*]

SUMMARY

Previous studies have focused on the impact of individual RNA modifications on tumor development. This study comprehensively investigated the effects of multiple RNA modifications, including m6A, alternative polyadenylation, pseudouridine, adenosine-to-inosine editing, and uridylation, on gastric cancer (GC). By analyzing 1,946 GC samples from eleven independent cohorts, we identified distinct clusters of RNA modification genes with varying survival rates and immunological characteristics. We assessed the chromatin activity of these RNA modification clusters through regulon enrichment analysis. A prognostic model was developed using Stepwise Regression and Random Survival Forest algorithms and validated in ten independent datasets. Notably, the low-risk group showed a more favorable prognosis and positive response to immune checkpoint blockade therapy. Single-cell RNA sequencing confirmed the abundant expression of signature genes in B cells and plasma cells. Overall, our findings shed light on the potential significance of multiple RNA modifications in GC prognosis, stemness development, and chemotherapy resistance.

INTRODUCTION

Gastric cancer (GC) is the fifth most prevalent type of malignancy and the fourth leading cause of cancer-related death worldwide, with a high incidence in East Asia, where half of the patients live.[1] Unfortunately, GC is often clinically advanced,[2] and patients present with a poor prognosis without effective treatment and medications.[3–5]

Epigenetic modifications are heritable modifications that regulate gene expression but do not change the sequence of DNA.[6] From the perspective of genetic aberrance, GC can be triggered by the accumulation of multiple somatic mutations in driver genes controlling key signaling pathways.[7,8] An increasing number of recent studies have shown that among the epigenetic modifications, alterations in RNA modifications have a significant role to play in the development of various human physiological disorders and malignant cancers.[9,10]

Currently, more than 170 RNA epigenetic modifications have been identified,[11] mainly including N6-methyladenosine (m^6A), polyadenylation alternative, pseudouridine,[12] etc.

m6A, the most prolific internal modification of RNA in eukaryotic cells, is involved in all aspects of RNA regulation, including transcriptional stability, pre-mRNA splicing, polyadenylation, mRNA export, and translation.[13] Its effects have gradually clarified on malignancies, such as breast cancer, hepatocellular carcinoma, pancreatic cancer, and prostate cancer.[14,15]

Alternative polyadenylation (APA), a common and important gene regulation phenomenon, can generate various transcript isoforms with different 3′ ends from the same gene.[16,17] Dysregulation of APA impacts the expression of proto-oncogenes and oncogenes, leading to the development and progression of various cancers,[18] with the process being influenced by various regulators,[19] including CFIm25, PCF11, and hnRNPC.

Adenosine-to-inosine (A-to-I) editing, a common mode of RNA modification, is translated by three enzymes of the ADAR family: the catalytically active ADAR1 and ADAR2, and the catalytically inactive ADAR3.[20]

Pseudouridine, the C5-glycoside isomer of uridine,[21] is able to modify different types of RNA.[22] Several studies showed that pseudouridine played functional roles in RNA biogenesis, structure, stability, and regulation of gene expression and mRNA structure.[23]

Uridylation, a common modification at the 3' RNA termini in eukaryotic cells, mainly promotes degradation in mRNAs.[24] TUT4 and TUT7, also known as ZCCHC11 and ZCCHC6, respectively, were identified as mRNA uridylation enzymes.[25]

[1]Department of Epidemiology and Biostatistics, Key Laboratory of Molecular Cancer Epidemiology, Key Laboratory of Prevention and Control of Human Major Diseases, Ministry of Education, National Clinical Research Center for Cancer, Tianjin Medical University Cancer Institute and Hospital, Tianjin Medical University, Tianjin 300060, China
[2]Department of Bioinformatics, The Province and Ministry Co-sponsored Collaborative Innovation Center for Medical Epigenetics, Key Laboratory of Immune Microenvironment and Disease (Ministry of Education), School of Basic Medical Sciences, Tianjin Medical University, Tianjin 300070, China
[3]These authors contributed equally
[4]Lead contact
*Correspondence: benliu100@tmu.edu.cn
https://doi.org/10.1016/j.isci.2024.108897

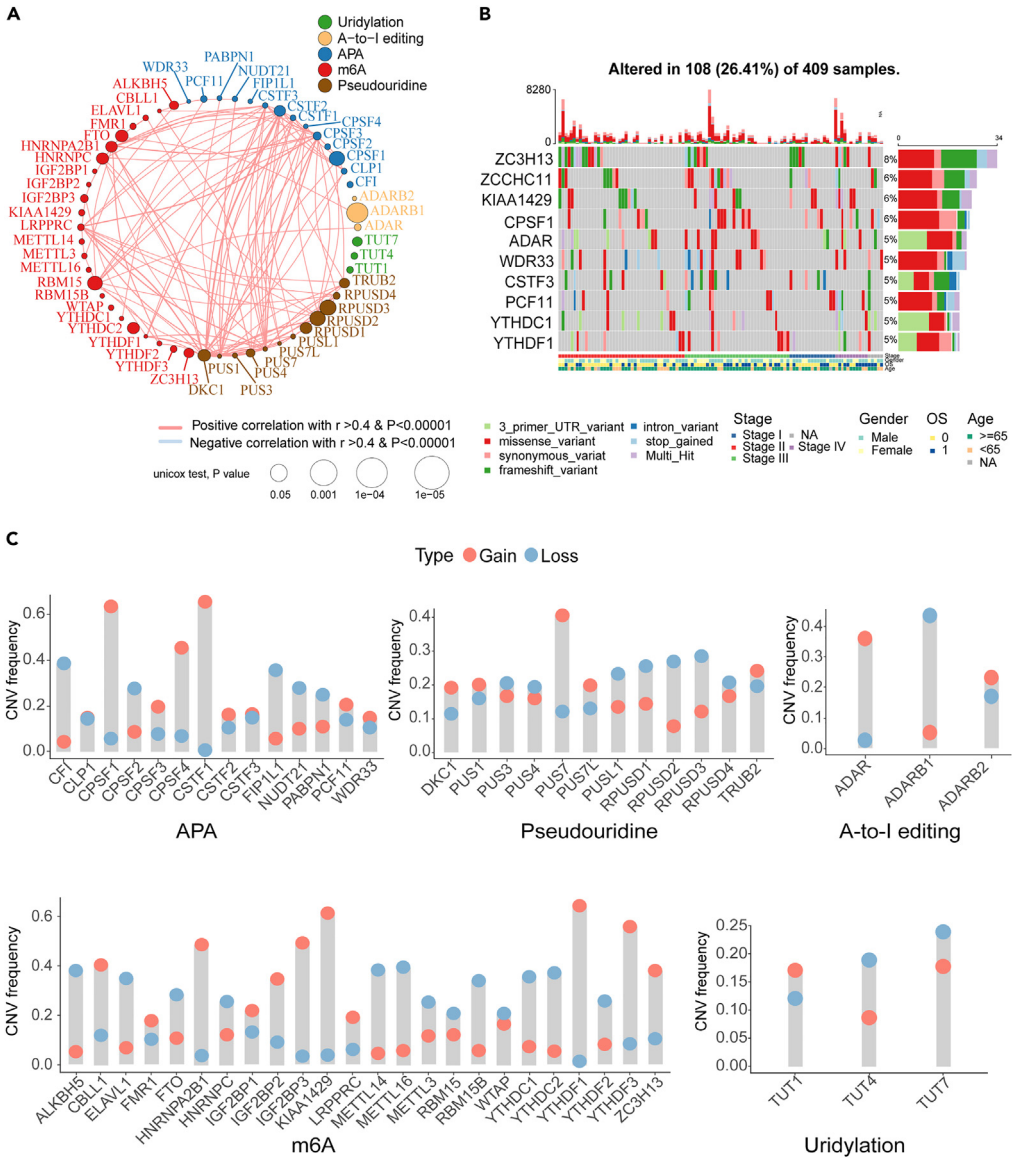

Figure 1. Bioinformatics analysis of the expression and genetic variation of five RNA modification subtypes

(A) The correlation between 56 RNA modifying enzymes.

(B) Waterfall diagram of the top ten mutated regulators. See also Figure S1.

(C) The CNV alteration of the 56 RNA modification regulators.

This study enrolled five common RNA modifications, including m^{6}A, A-to-I-editing, APA, pseudouridine, and uridylation. Then we collected GC samples from eight independent GC cohorts for analysis and identified three subtypes differing in prognostic characteristics, immune infiltration, and modification enzymes. Meanwhile, we constructed a risk signature consisting of 24 RNA modification-related genes and verified it in ten independent GC cohorts and an immune checkpoint blockade (ICD) cohort to prove that this signature can predict patient prognosis, immune characteristics, and therapeutic efficacy of GC.

RESULTS

Genetic variation mapping of RNA-modifying enzymes in gastric cancer

By Spearman correlation analysis, we found a significant positive pairwise correlation in the vast majority of the expression level of 56 RNA modifying enzymes. The correlations of regulatory enzymes existed between the same RNA modification types and different types, suggesting an association between different RNA modifications, including m6A, A-to-I-editing, APA, pseudouridine, and uridylation (Figure 1A). Thus, it is necessary to combine and analyze these RNA-modifying enzymes together.

In the TCGA-STAD cohort containing 409 samples, 56 RNA modifying enzymes were mutated according to the mutational information (Figure S1). The waterfall plot showed the gene mutation ratio in these samples, and we determined the top 10 significantly different mutation genes, including ZC3H13, ZCCHC11, KIAA1429, CPSF1, ADAR, WDR33, CSTF3, PCF11, YTHDC1, YTHDF1 (Figure 1B). The copy number variation (CNV) revealed the regulators' copy number changes (Figure 1C). Most APA regulators displayed deletion in copy number, except for CPSF1, CPSF4, and CSTF2. Most pseudouridine regulators displayed copy number deletion, except for PUS7. ADAR in A-to-I editing regulators showed significant amplification, whereas ADARB1 showed deletion. In m6A regulators, CBLL1, HNRNPA2B1, IGF2BP3, KIAA1429, YTHDF1, YTHDF2, and ZC3H13 showed copy number amplification, and ALKBH5, ELAVL1, FTO, METTL4, METTL6, RBM15B, YTHDC1, and YTHDC2 showed copy number deletion. Most uridylation regulators are displayed in copy number deletion, except for TUT1.

Gastric cancer subtypes with different RNA modification and prognosis patterns

By a supervised clustering algorithm with survival information weight, we integrated eight datasets (TCGA-STAD, GSE13861, GSE15459, GSE26899, GSE62254, Tianjin, GSE34942, GSE26901) as a whole as the training cohort for the subtype analysis, classified GC patients into three subtypes (named cluster1, cluster2, cluster3) with different RNA modification patterns based on the expression of 56 RNA modification regulatory enzymes (Figures 2A and 2B, and Tables S2–S4). The prognosis between the three subtypes showed a significant difference ($p = 0.0019$): cluster1 presented the best prognosis, while cluster2 and cluster3 were poorer than cluster1 (Figure 2C). To demonstrate the stability of the subtypes, we validated the previous subtypes in another combined dataset (GSE57303, GSE84437), yielding three subtypes with different RNA modification patterns, which also remained statistically significant prognostic differences ($p = 0.0089$) (Figures 2D–2F).

In order to exclude the confounding factors related to survival outcomes, we adjusted gender, age, and clinical stage on a multifactorial Cox regression model for survival analysis, showing that cluster3 was still an independent prognostic factor whose patients had a worse prognosis, which indicated that RNA modification difference was independent of clinical indicators such as age and staging (Figures 2G and 2H). Heatmap revealed differences in the expression of RNA modifying enzymes between three subtypes and found that cluster1 had higher expression levels of RNA modifying enzyme (Figures 2I, and S2).

Different characteristics of immune infiltration and biological features in three clusters

We further evaluated the correlation between RNA modification and immune infiltration, including immune score, stromal score, tumor purity, and infiltrating abundances of 28 immune cells. The result suggested that the abundance of immune infiltration differs between subtypes, with cluster1 having the highest tumor purity score (Figure 3A). However, the lowest stromal score, immune score, and Estimation of STromal and Immune cells in MAlignant Tumor tissues using Expression data (ESTIMATE) score (Figures 3B–3D) compared to cluster2 and cluster3, which showed poorer prognosis. Furthermore, the infiltrating abundances of 28 immune cells demonstrated that cluster3 had a remarkable infiltration of immune cells (Figure 3F). Similar to previous conclusions, the cluster3 was characterized by the highest immune score and immune cell infiltration in the validation cohort (Figure S3).

Furthermore, the mRNAsi results for the three clusters showed completely opposite trends to the immune, stromal, and ESTIMATE scores, but followed the same trend as for tumor purity, indicating that the level of immune and stromal cell infiltration decreases with increasing GC stemness ($p < 0.0001$, Figure 3E). More specifically, cluster1 had the highest mRNAsi, and therefore patients in this group had the highest degree of tumor dedifferentiation. The same results were obtained in the validation set (Figure S4). We also utilized TIMER, CIBERSORT, ESTIMATE, MCP counter, and single sample gene sets enrichment analysis (ssGSEA) algorithms to assess the abundance of tumor immune infiltration. The heatmap showed the landscape of immune infiltration based on these five algorithms (Figure 3G).

Different transcriptional regulation patterns among three clusters

Given the close correlation between regulator activity and RNA modification subtypes, we conducted the regulon analysis consisting of 9 GC-specific transcription factors (TFs) and 56 RNA modifying enzymes in multiple RNA modification subtypes (Figure 4A), as well as the activity of potential regulators associated with cancer chromatin remodeling (Figure 4B), providing strong confirmation of the biological relevance of the three clusters.

Cluster1 is accompanied by activation of regulators such as SOX9, HNF4A, EHF, ELF3, and KLF5, while cluster2 and cluster3, which are completely different from cluster1, are characterized by similar transcriptional regulatory activity, dominated by MECOM, KLF3, CREB3L1, and AHR. Differences in the activity of regulators associated with cancer chromatin remodeling provided further evidence that these RNA modification subtypes were molecularly distinct. Compared to cluster1 and 2, genes from the MYST family associated with histone acetyltransferases (HATs) showed overexpression in cluster3. Of the HDAC family genes associated with histone deacetylases, class I is overexpressed in cluster1, such as HDAC1 and HDAC8, while classes IIA and III are overexpressed in cluster3, such as HDAC4, HDAC5, SIRT1, SIRT6, and SIRT7. These results suggested that different RNA modification subtypes may have mutual interactions with transcriptional regulation and chromatin modification.

Construction of RNA modification-related prognostic signature

In order to better predict prognosis and guide treatment, we identified 24 differentially expressed genes (DEGs) for constructing an RNA modification-related model, including PPP1R14A, ACTG2, TUBB6, MMACHC, KCNMB1, MYOT, MATN2, SBSPON, MANEAL, FLNA, TNFRSF17, HELLS, PTCHD1, CENPN, UNG, RRM1, CDC25B, CCNB2, PAICS, EPHB2, PMP22, RNASEH2A, ODC1, NRXN3 (Table S5).

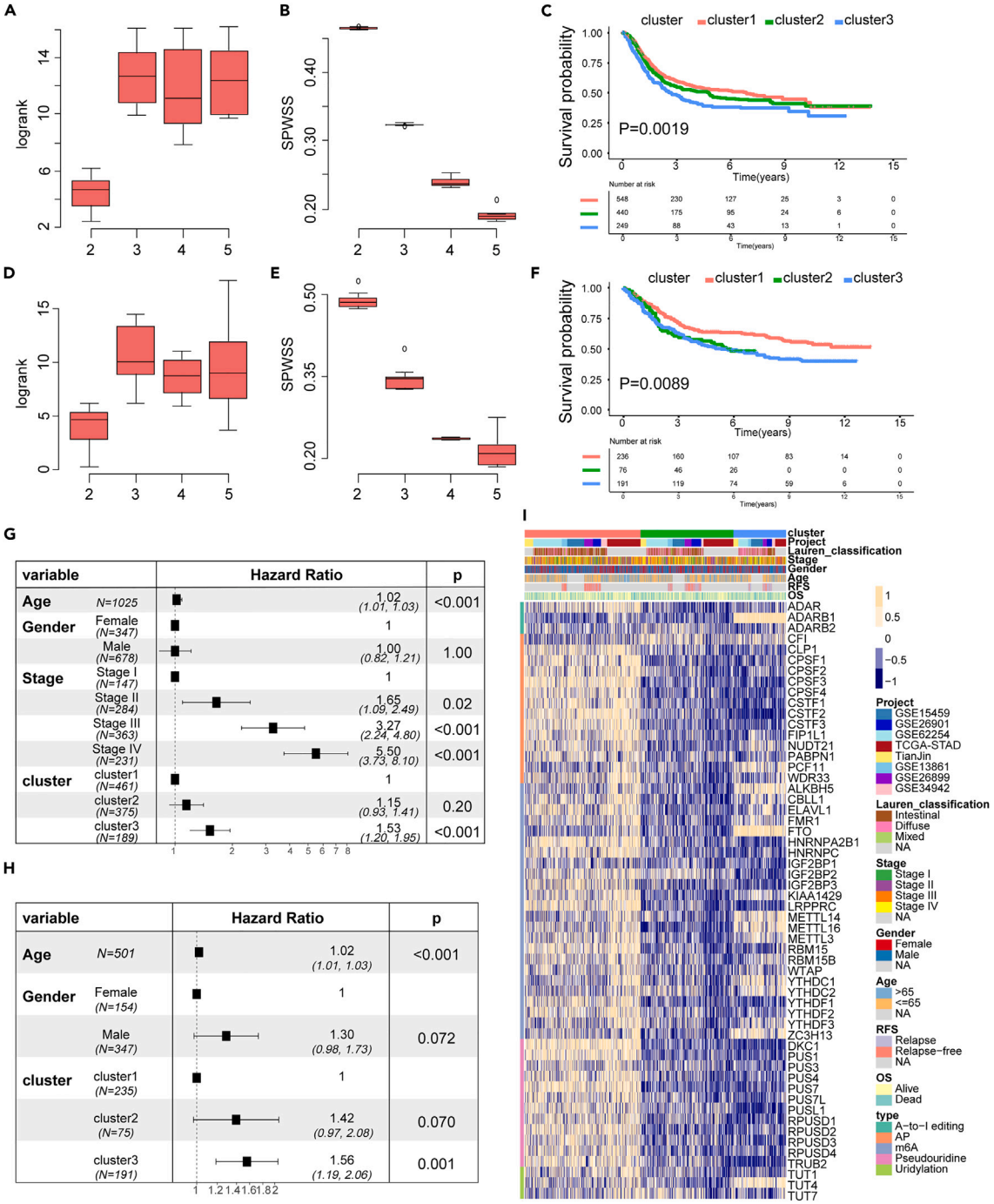

Figure 2. Identification of consensus clusters by 56 RNA modification regulators

(A and D) Log rank test statistics of training set and verification set.

(B and E) Standardized intra-cluster sums of squares calculated by cross-validation of the training set and verification set.

(C and F) Kaplan-Meier curves for survival prediction of patients in the three clusters of set and verification set.

(G and H) Forest plot representation of the multivariate Cox regression analysis of risk signature with age, gender, and tumor stage was taken into account.

(I) Expression levels of 56 RNA modification enzymes between three clusters. Data with error bars were presented as mean (SD). See also Figure S2.

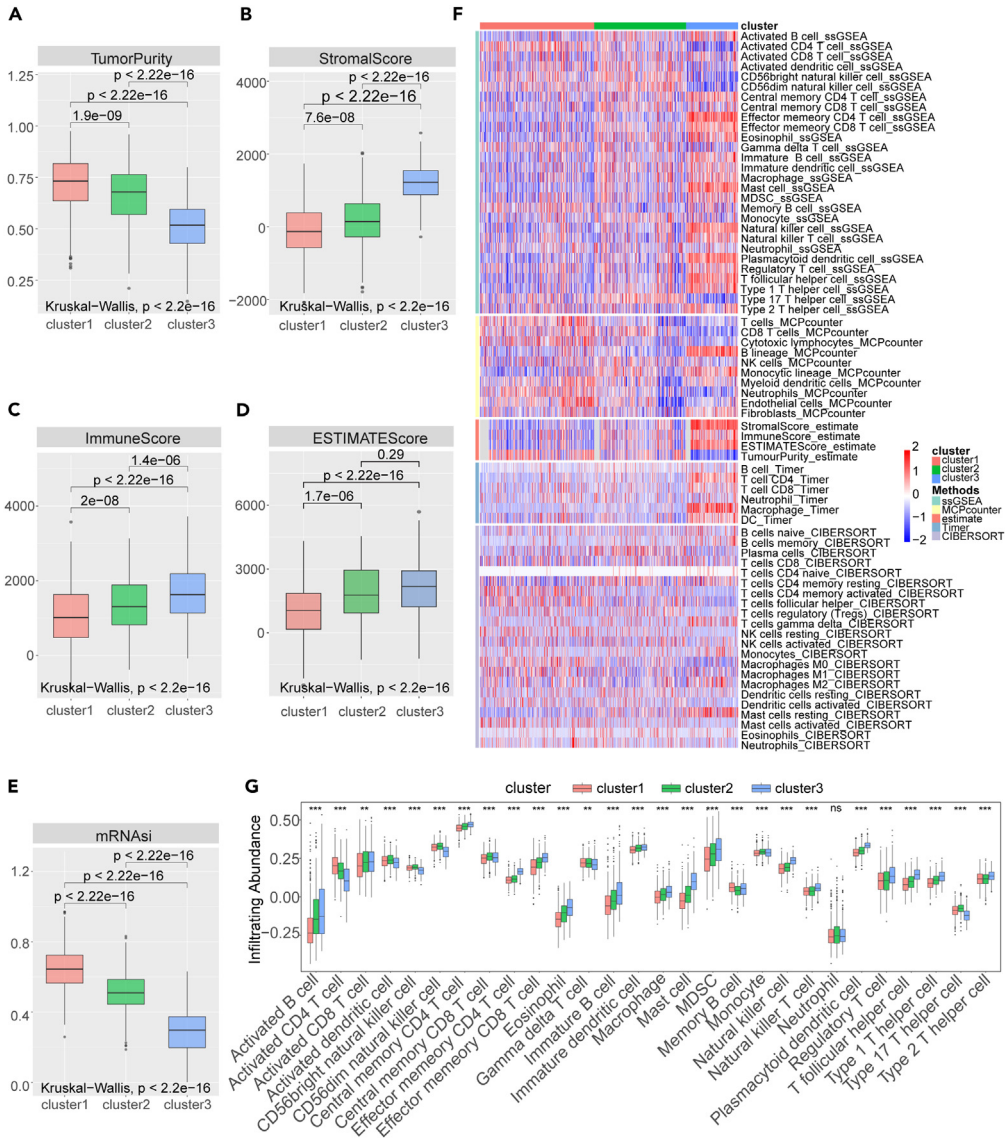

Figure 3. The three RNA modification clusters showed differential immune infiltration

(A) Tumor purity in GC samples was compared between the three clusters.

(B) Stromal scores in GC samples were compared between the three clusters.

(C) Immune scores in GC samples were compared between the three clusters.

(D) ESTIMATE scores in GC samples were compared between the three clusters.

(E) mRNAsi in GC samples were compared between the three clusters.

(F) Infiltrating abundances of 28 immune cells between the three clusters.

(G) The landscape of immune infiltration is based on TIMER, CIBERSORT, estimate, MCP counter, and ssGSEA algorithms. Data with error bars were presented as mean (SD). See also Figures S3 and S4.

Next, we identified the value of risk signature in predicting the outcome of GC patients. After fitting, a risk score was obtained for each sample, and patients in the cohort were divided into two groups, high- and low-risk groups, based on the best cut-off values. Kaplan-Meier survival analysis showed that patients in the low-risk score group had a significantly better prognosis than those in the high-risk score group (long-rank test, $p < 0.0001$; Figure 5A). The previous results were also validated in ten independent external validations (long-rank test, $p < 0.05$; Figures 5B–5F, and S5), in which three cohorts showed significant differences in the prognosis of recurrence-free survival (RFS) between high- and low-risk groups (long-rank test, $p < 0.05$; Figure 5G).

Then we included clinical variables such as gender, age, and stage in a multivariate Cox regression model to verify whether the prognostic model was an independent factor after excluding the influence of confounding factors on prognosis. The results suggested that the

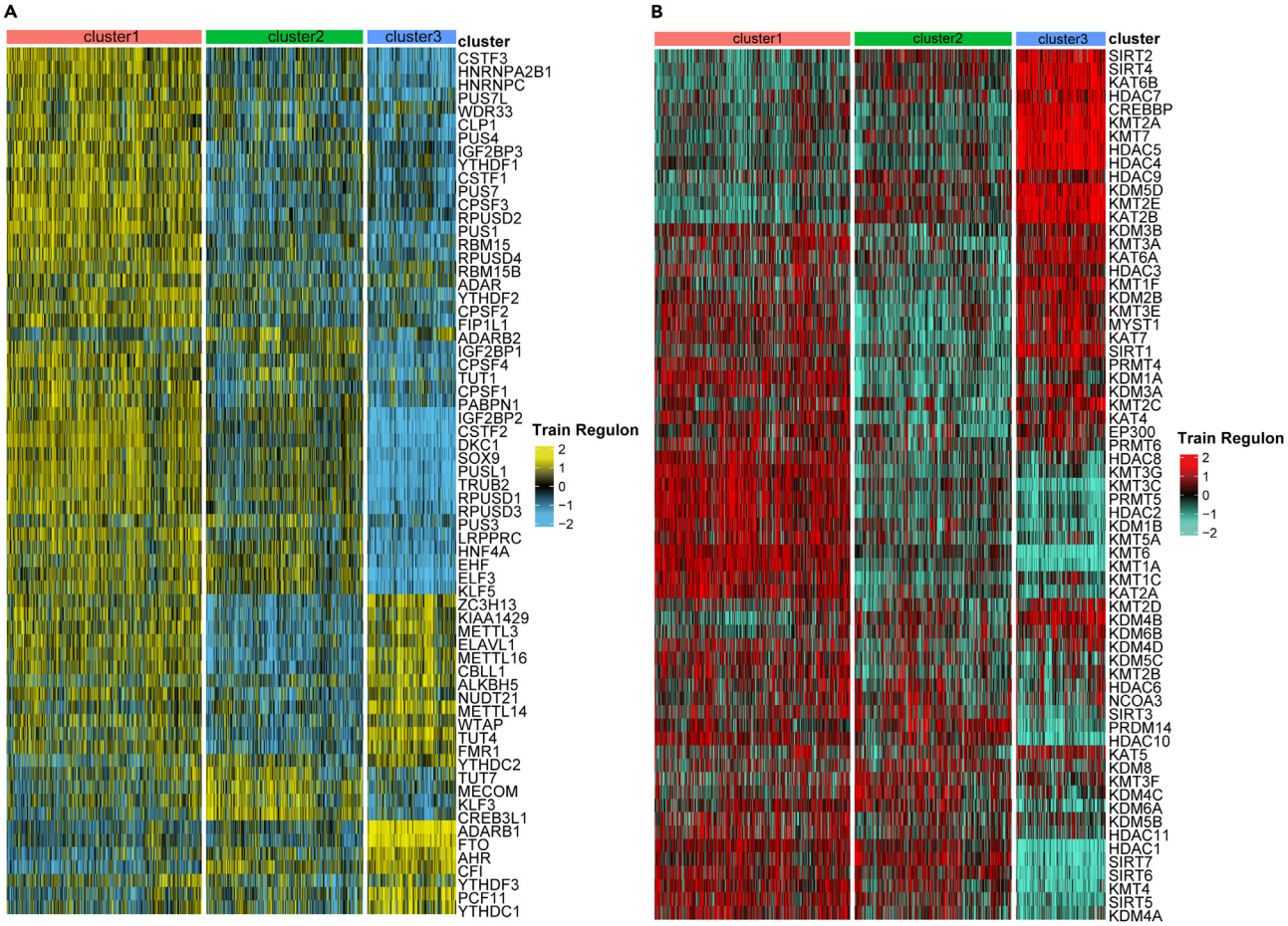

Figure 4. The chromatin activity of three RNA modification clusters

(A) The activity of a transcriptional regulatory network consisting of nine gastric cancer-specific transcription factors and 56 RNA-modifying enzymes.

(B) The activity of histone-modifying regulators associated with chromatin remodeling in cancer.

prognostic model remained an independent prognostic factor, and this result was also validated in five of the ten independent GC datasets (Figures 5A–5F). Hence, the risk signature could be an independent prognostic factor for GC patients.

The association between risk signature and immune infiltration in GC

We utilized the ESTIMATE algorithm to compute the immune score, stromal score, and tumor purity (Figures 6A–6D). The Boxplot analysis showed that a significant positive correlation existed between the high-risk group and ESTIMATE score and stromal score, respectively. However, a negative correlation existed between the high-risk group and tumor purity. Furthermore, the high-risk group exhibited a lower immunophenoscore (IPS) than the low-risk group, but there was no statistical difference (Figure 6F). In addition, we found that the infiltrating abundances of 28 immune cells in the two groups differed (Figure 6E). The low-risk group showed a higher infiltration of activated $CD4^+$ T cells, activated $CD8^+$ T cells, and activated dendritic cells. However, the high- and low-subgroups only showed a statistically significant difference for activated $CD4^+$ T cells. Moreover, the infiltration of activated B cells was slightly higher in the high-risk group than in the low-risk group.

Then we performed a gene set enrichment analysis (GSEA) enrichment analysis. Gene ontology (GO) enrichment analysis showed that patients in the high-risk group were mainly enriched in pathways related to malignant tumor cells proliferation, metastasis, and invasion, including platelet-derived growth factor (PDGF) binding, chondrocyte morphogenesis, and interstitial matrix (Figure 6G). In comparison, Kyoto Encyclopedia of Genes and Genomes (KEGG) enrichment analysis showed that the high-risk group was prominently related to the pathways of cellular physiology, environment and state, including the cGMP-PKG signaling pathway and focal adhesion (Figure 6H). In addition, compared to the high-risk group, further GO enrichment analysis revealed that the low-risk group was mainly related to cell cycle and cellular differentiation, such as chromatin remodeling at the centromere, DNA replication checkpoint, and minichromosome maintenance (MCM) complex. KEGG enrichment analysis showed that the low-risk group's association with cancer nutrition and metabolism-related pathways, such as aminoacyl-tRNA biosynthesis, arginine biosynthesis, citrate cycle (also known as TCA cycle), and fructose and mannose metabolism (Figure S6).

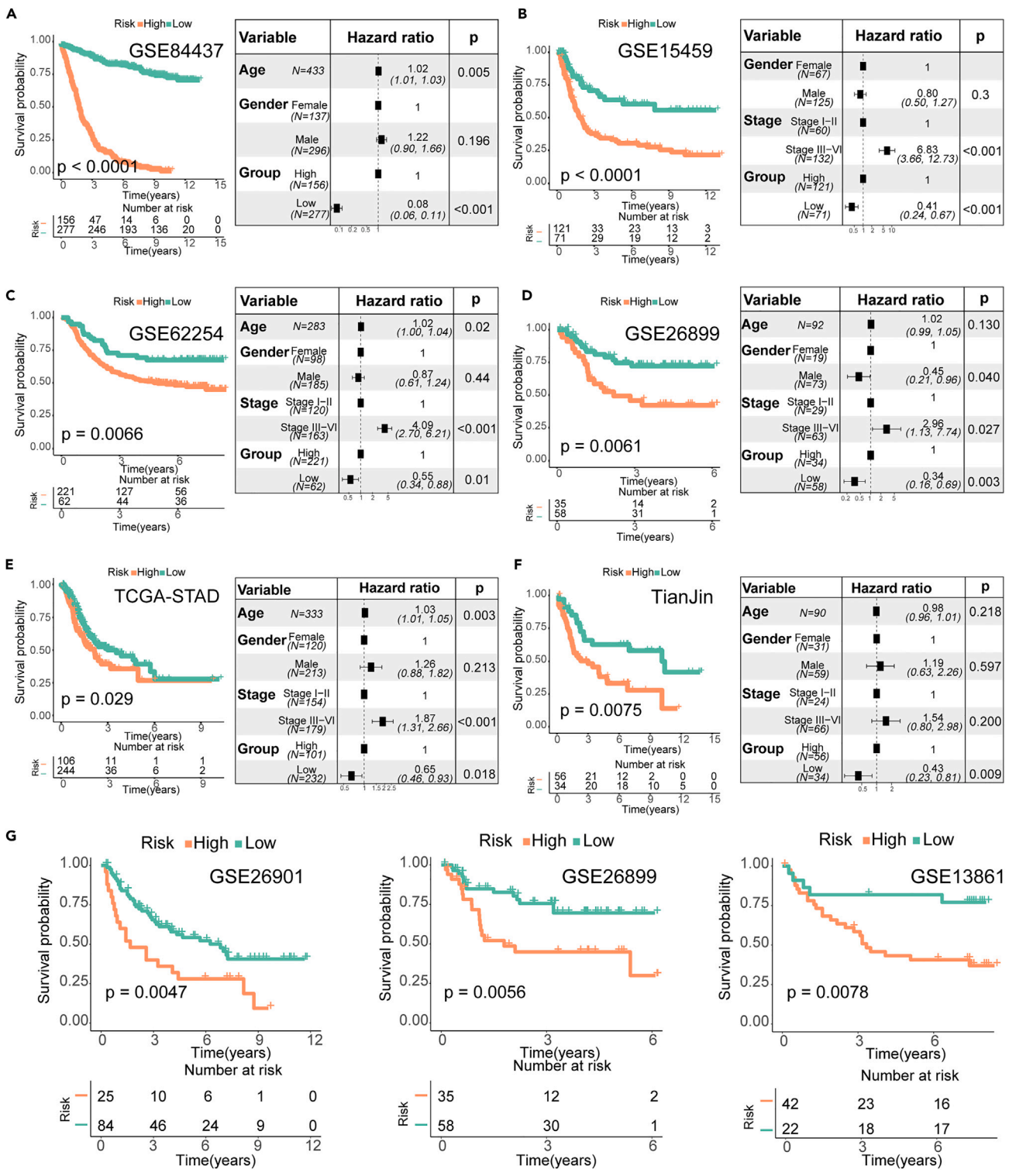

Figure 5. Survival analysis of the RNA modification-related signature

Kaplan-Meier curves for survival prediction in high- and low-risk score groups of gastric cancer (Left). Forest plots representing the multivariate Cox regression analysis of RNA modification-related signatures with age, gender, and tumor stage were taken into account (Right). See also Figure S5.

Figure 5. *Continued*

(A) Training set-GSE84437 (HR=0.08, 95% CI: 0.06-0.11, p < 0.001), (B) Validation set-GSE15459 (HR=0.41, 95% CI: 0.24-0.67, p < 0.001), (C) Validation set-GSE62254 (HR=0.55, 95% CI: 0.34-0.88, p = 0.01), (D) Validation set-GSE26899 (HR=0.34, 95% CI: 0.16-0.69, p = 0.003), (E) Validation set-TCGA-STAD (HR=0.65, 95% CI: 0.46-0.93, p = 0.018), (F) Validation set-Tianjin (HR=0.43, 95% CI: 0.23-0.81, p = 0.009).

(G) Kaplan-Meier curves for recurrence-free survival prediction in high- and low-risk score groups of gastric cancer of GSE26901, GSE26899, GSE13861. See also Figure S5.

The role of RNA modification-related signature in immune-checkpoint blockade cohort

To further test the predictive efficiency and patients' responsiveness to the risk signature in immunotherapy cohorts, we analyzed the proportion of patients with response to ICD therapy in low- and high-risk groups. The results showed that the model was independently validated in a uroepithelial cancer cohort named IMvigor210. In alignment with previous findings, patients in the low-risk group of the uroepithelial cancer cohort had a better prognosis and a higher immunotherapy response rate than the high-risk group (Figures 6I and 6J).

Distribution of RNA modification-related genes in the single-cell atlas

We obtained the scRNA-seq dataset (GSE167297) from GEO, classified 30,365 GC cells into nine clusters, and annotated the cell types using canonical marker genes (Figures 7A and 7B). Then, we performed gene enrichment analysis of the 24 DEGs identified using AUcell. The results showed that among these nine major cell populations in a single-cell atlas of multi-regional GC cells, RNA modification-related genes appeared to be hyper-abundantly expressed in B cells and plasma cells (Figures 7C–7E). Based on the gene expression dynamics of B cells and plasma cells, we contrasted a pseudotime analysis and determined an independent branchpoint (Figure 7F). The gene expression pattern across pseudotime displayed that the expression curves of TNFRSF17 and ODC1 changed more significantly. In the later stage, the expression of TNFRSF17 showed a significant increase before the decrease, while that of ODC1 was relatively smooth descending and then ascending (Figure 7G).

DISCUSSION

It is imperative to identify the impact of different RNA modification patterns on immune cell infiltration to guide more effective individual GC treatment. The present study integrated genomic information from 1,740 GC samples to comprehensively assess and correlate RNA modification subtypes with TME cell infiltration characteristics. We incorporated 5 RNA modification patterns, including m6A, APA, A-to-I editing, pseudouridine, and uridylation, to reveal the overall and particular interactions of RNA modification at an epigenetic level in GC. Among regulators with notable mutations, previous studies have indicated a high mutation rate in GC for ZCH3H13 and KIAA1429.[20] These two m6A regulators, combined with METTL3, form a protein complex that regulates cancer transcription, maturation, localization, translation, and degradation, improving the stability of pathogenic mRNAs in GC. ADAR1 and ADAR2, the writers of A-to-I editing and also editors, are closely related to GC prognosis. This effect is carried out by ADAR-induced RNA misediting: upregulation of ADAR1 or downregulation of ADAR2 alone leads to a favorable prognosis; upregulation of both together leads to a dismal prognosis.[26,27] Substantial factual evidence suggests that multiple m6A regulators, such as FTO and YTHDF1, can be critical targets for cancer therapy. As several of the previous studies have shown that RNA-modifying enzymes affect GC, we considered the synthesis and interactions of these enzymes in an integrated manner and carried out the following thorough study.

Instead of the single unsupervised clustering algorithm previously used, we conducted the supervised clustering model incorporating survival information to type multiple cohorts of GC patients. We identified three distinct RNA modification subtypes with different immune infiltration characteristics, suggesting that RNA modifications play a non-negligible role in shaping individual TME characteristics. Cluster1, with higher levels of modified enzyme expression and better prognostic outlook, showed the lowest stromal and immune scores, the highest tumor purity, and the mRNAsi score. Currently, available studies have not reached a unified conclusion on the prognostic significance of mRNAsi in GC.[28–30] Higher mRNAsi was associated with reduced immune infiltration and PD-L1 expression in adrenocortical carcinoma (ACC), esophageal squamous cell carcinoma (ESCC), and esophageal adenocarcinoma (ESAD), ultimately leading to a more unfavorable prognosis.[31,32] However, Guo et al. found that mRNAsi showed a tendency for higher mRNAsi scores, shorter overall survival (OS), and worse prognosis in both intestinal-type GC (IGC) and diffuse-type GC (DGC), which was similar to our results. The aforementioned results suggest that the relationship between mRNAsi scores and the pathological types and immunophenotyping of GC deserves further investigation. Since there were significant differences in mRNAsi among clusters, we focused on stemness signaling pathways-related TFs in the signature. The main characteristics of cancer stemness include tumorigenesis, metastasis, tumor self-renewal ability, cancer metabolism reprogramming, and tumor immune microenvironment remodeling.[33] Previous studies have shown that multiple RNA modifying enzymes, by regulating stemness signaling pathways such as Notch, WNT, Hedgehog (HH), and Hippo in cancer stem cells (CSCs), exerting influences on GC proliferation and invasion.[34–36] Given that tumor-initiating stem cells suppress cytotoxic T cell responses through surface molecules of CD80,[37] the interaction of tumor stemness with RNA modifications may be critical for activating immune checkpoint therapeutic pathways. These aforementioned results converged with the findings of previous studies of GC.[38]

Chromatin histone modification regulatory networks differed among three clusters, revealing an association between multiple RNA modification patterns and chromatin modifications. Several studies have shown that RNA-modifying enzymes direct gene regulation through a co-transcriptional mechanism and can target DNA through chromatin modifications, affecting epigenetic regulation.[39] The RNA that emerges during RNA polymerase II (Pol II) transcription, "nascent RNA", antagonizes interactions of a set of transcriptional regulators with chromatin,

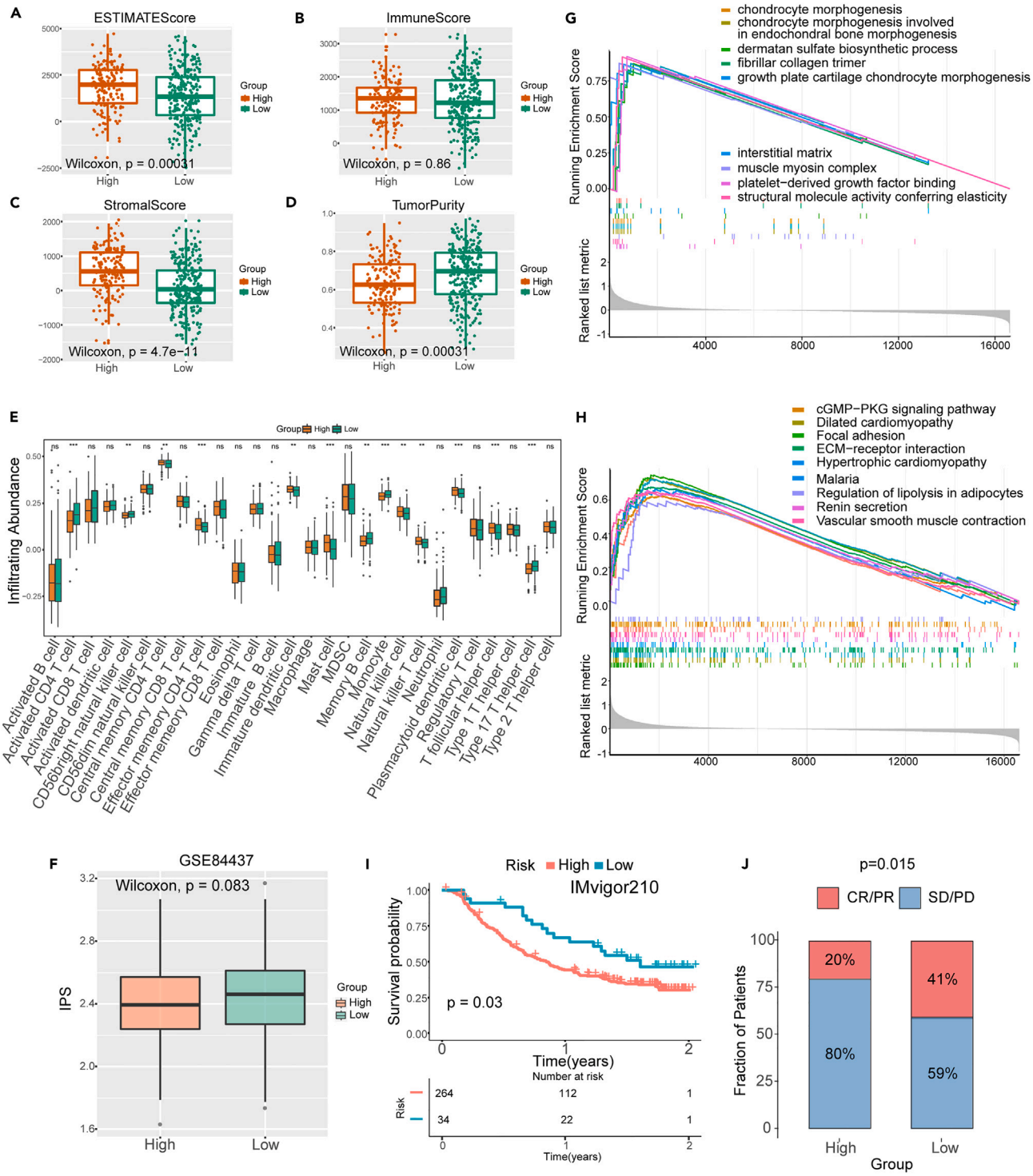

Figure 6. Validation of the RNA modification-related risk signature

(A) The difference in ESTIMATE scores between high- and low-risk groups.

(B) The difference in immune scores between high- and low-risk groups.

(C) The difference in stromal scores between high- and low-risk groups.

(D) The difference in tumor purity between high- and low-risk groups.

(E) Infiltrating abundances of 28 immune cells were compared between the high- and low-risk groups (*p < 0.05, **p < 0.01, ***p < 0.001).

(F) The difference in IPS between high- and low-groups.

Figure 6. *Continued*

(G) Gene ontology (GO) analysis of the high-risk group compared to the low-risk group. See also Figure S6.

(H) The Kyoto Encyclopedia of Genes and Genomes (KEGG) analysis of the high-risk group compared to the low-risk group. See also Figure S6.

(I) Kaplan Meier plots of patients treated with immune checkpoint blockade in uroepithelial cancer cohort IMvigor210.

(J) CR, complete response; PR, partial response; SD, stable disease; PD, progressive disease. Data with error bars were presented as mean (SD).

regulating the transcription process.[40] Moreover, m6A methylation on chromosome-associated regulatory RNAs (carRNAs) can collectively regulate chromatin state and transcription. Liu J et al. showed that reducing m6A methylation by METTL3 depletion promoted open chromatin state and downstream transcription.[41] The epigenetic regulatory function of RNA modification is also related to the involvement of RNA-binding proteins (RBPs) and chromatin-associated proteins (CAPs). RBPs may enhance chromatin network interaction by harnessing regulatory RNAs to control transcription. For example, RBM25, an RBP involved in splicing regulation, and its depletion attenuates the activities of chromatin binding, DNA looping, and transcription depending on YY1, a known RNA-dependent TF.[42] D GH et al. suggested CAPs had a dual nucleic acid affinity and could unify RNA-mediated chromatin regulation of transcription with chromatin-mediated post-transcriptional regulation of RNA.[43] All of the previous evidence hints that RNA modifications are intricately linked to chromatin regulation, which deserves an in-depth investigation of the underlying epigenetic mechanisms.

For better-personalized guidance of patient prognosis, we utilized machine learning and Cox regression to construct a prognostic signature that predicted patient immune response, drug responsiveness, and validated it in multiple immunotherapy cohorts. Based on 24 DEGs, RNA modification-related signature was constructed and validated. GC patients were divided into low-and high-risk groups, showing distinct prognoses and TME characterization. The high-risk group showed more innate immune cells and cellular stroma, with PDGF, focal adhesion, and cGMP-PKG signaling pathway activation, which have been proven to induce angiogenesis, malignant proliferation, self-renewal, and metastasis.[44–47] Recent studies demonstrated that PRTG (ZEB1 upregulated protein) activates cGMP/PKG axis to promote GC cell proliferation, metastasis, and chemoresistance.[48] Therefore, blocking the cGMP/PKG axis could be considered as a promising GC therapeutic strategy. The low-risk group showed more activated immune cells, such as activated $CD4^+$ and activated $CD8^+$ T cells, with characteristics of a hot tumor.[49] The low-risk group also presented a higher IPS, which predicts a better response of the patients to immunotherapy.[50] GO analysis showed that the MCM complex pathway significantly enriched the low-risk group. It has been shown that YTHDC1 (an m6A reader) regulates acute myeloid leukemia (AML) by affecting DNA regulators, also known as the MCM complex.[51] Thus, this suggested that RNA modifications could influence cancer pathogenesis by affecting DNA replication.

Furthermore, we found associations between the low-risk group and biosynthetic and metabolic pathways via pathways enrichment analysis. TME interacts with certain trophic metabolic pathways to regulate cancer growth, invasion, and immune escape. Kim et al. showed that high levels of lysyl-tRNA synthetase (KRS, an aminoacyl-tRNA synthetase) in tumor-associated inflammatory (TAI) cells in GC were associated with better prognostic survival, suggesting that KRS could be used as a potential biomarker for GC.[52] Arginine induces apoptosis, reducing cell growth in a human GC cell line but maintaining invasive cell potential.[53] Moreover, as a platinum medicine-sensitive tumor, GC shows overexpression of the enzyme argininosuccinate synthetase (ASS1) due to regulation by pro-inflammatory factors,[54] demonstrating a relationship between metabolome and inflammatory TME. TCA cycle intermediates can impact GC by modulating cellular activities, including metabolism and signaling,[55] and this process is regulated by short-chain fatty acids.[56] By inhibiting proliferation and increasing death, mannose supplementation has anti-cancer effects in non-small cell lung cancer (NSCLC).[57] This evidence suggests that we need to combine RNA modification-related signature with the metabolome in GC to provide more possibilities for exploring immunotherapy and improving prognosis. This needs to be validated by more studies.

We also elucidated the signature's efficacy by subsequent immune-checkpoint blockade cohort analysis. In this anti-PD-L1 cohort IMvigor210,[58] patients with a low-risk group of RNA modification-regulated signature demonstrated remarkable clinical benefit, prolonged survival, and treatment advantages. As one of the most common RNA modifications, the role of m6A modification on tumor therapy can be reflected in m6A modification-based targeted drugs. For example, small molecule inhibitors of the m6A demethylase Alkbh5 contributed to enhancing the efficacy of melanoma immunotherapy. Inhibitors of FTO, an important m6A demethylase, showed growth inhibitory effects on a variety of tumor cell lines, such as AML cell lines, melanoma cell lines, lung cancer cell lines, and glioblastoma, indicating the potential of FTO inhibitors for the treatment of cancer.[59,60] In addition, RNA modifications can also affect the effectiveness of existing conventional treatment regimens. RNA-modification regulators affect the sensitivity or resistance of cancer cells to chemotherapy drugs by interfering with various cellular activities, including glycolysis,[61] cellular autophagy, DNA damage,[62] and signaling pathways such as JAK2/STAT3 and Wnt/β-catenin signaling pathway.[63,64] However, the development of RNA modification-based treatments is mainly limited to common modification pathways, such as m6A and m5C, and research on GC is still lacking.

Single-cell and pseudotime analysis demonstrated that the signature genes were mainly expressed in B cells and plasma cells, and the gene expression of TNFRSF17 and ODC1 changed more significantly during the transformation of B cells to plasma cells. TNFRSF17, i.e., B cell maturation antigen (BCMA), proved to be an attractive target for chimeric antigen receptor T cell (CAR-T) therapy, since it is expressed only by subpopulations of normal and malignant plasma cells and mature B cells.[65,66] TNFRSF17 has now been identified as a novel therapeutic target for multiple myeloma and colon cancer sensitive to immunotherapy.[67,68] Claudin18.2 (CLDN18.2)-redirected CAR T therapy has been shown to show favorable anti-GC efficacy in the preclinical study.[69] Thus, we can hypothesize that BCMA is expected to facilitate the development and application of CAR-T therapy in GC by regulating the epigenetic mechanism of multiple RNA modifications. ODC1, the first rate-limiting enzyme in the polyamine biosynthetic pathway,[70] is an MYCN-mediated downstream target gene.[71,72] Raised expression of ODCI and MYCN induces proliferative migration of cancer cells through various cell signaling pathways, such as the hedgehog signaling

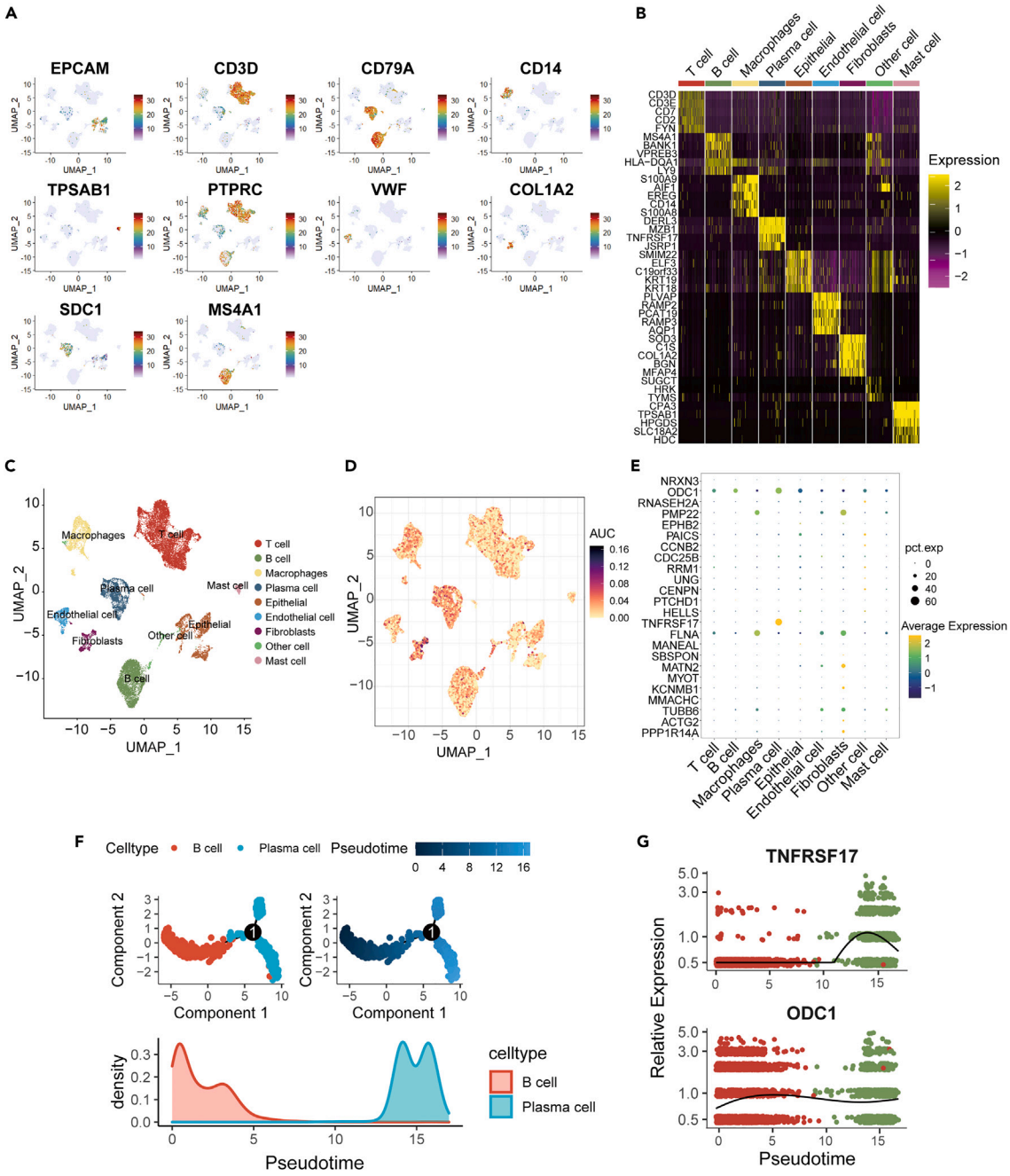

Figure 7. Major cell lineages and pseudotime analysis in the single-cell atlas

(A) Selected UMAP feature plots showing RNA expression of major nine cell lineages.

(B) The heatmap of the marker genes of the nine major cell lineages.

(C) UMAP plot showing the identified cell types of all immune cells.

(D) Gene enrichment of RNA modification-related genes used to construct signature was analyzed by AUCell.

(E) Bubble heatmap showing expression of RNA modification-related genes in nine major cell lineages. In a given cell identify, the sizes of circles indicate the percentage of the cells expressing each marker gene; The shades of green indicate the average expression of each gene.

(F) Pseudotime trajectory of B cells and plasma cells inferred by monocle, with each point colored by cell type (left) and pseudotime (right), and cluster distribution density along pseudotime (down).

(G) Jitter plots show the expression level of the genes changing with pseudotime. TNFRSF17 and ODC1 were among the most significantly upregulated genes in cells with larger pseudotime.

pathway, which predicts adverse outcomes in a variety of malignancies.[73–75] Therefore, according to integrated studies, we regarded RNA modification signature as an independent, reliable, and robust biomarker of GC that can provide precise and comprehensive guidance for individual immunotherapy strategies.

At present, the function and mechanism of non-coding RNAs, especially long non-coding RNAs (lncRNAs) and enhancer RNAs (eRNAs), have received extensive attention, and RNA modification of non-coding RNAs has become a promising research direction for the future. Metastasis-associated lung adenocarcinoma transcript (MALAT1) is a lncRNA whose dysregulation has been associated with the progression of various cancers,[76] and the m6A modification can act as a structural switch to affect its interaction with proteins by regulating the structure of MALAT1. ABL is a lncRNA highly expressed in GC, the overexpression of which inhibits GC apoptosis, promotes GC cell survival, and leads to multidrug resistance. The m6A modification that occurs in ABL is mediated by METTL3, which further maintains ABL stability by binding to the RBP IGF2BP1.[77] An RNA modification study of eRNAs shows that m6A-methylated eRNAs label highly active enhancers, recruit the nuclear m6A reader YTHDC1 for phase separation, and regulate enhancer activation and gene transcription.[78] In addition, m6A on bone-specific eRNAs was shown to play a post-transcriptional functional role in bone mPCa and correlated with radiotherapy (RT) tolerance.[79] In summary, we propose to focus our future research on the RNA modification of eRNAs, which is expected to better decipher the mechanism of cancer development at the epigenetic level.

Conclusions

In conclusion, this study integrated five RNA modification patterns, including m6A, APA, A-to-I editing, pseudouridine, and uridylation, and explained the integration and interaction of regulator networks on TME and prognosis. We also established a reliable prognostic model, analyzed the biological effects of this model, and demonstrated the relevance of the model for directing individualized immunotherapy.

Limitations of the study

Still, there are certain limitations to our study. First, data heterogeneity was inevitable as every cohort was gathered from several online platforms. Second, this study lacks clinical and experimental validation of the results. Additionally, we chose 28 immune cells to analyze immune infiltration, and additional algorithms to predict immune infiltrating cells are further required. Finally, we have employed an immunotherapy cohort for malignant uroepithelial carcinoma to validate the immunotherapy response. However, a prospective ICI therapy cohort for GC is still required. More experiments are needed to elucidate the potential molecular and pathogenic mechanisms of RNA modifications and their regulators in tumor progression and immunotherapeutic applications.

STAR★METHODS

Detailed methods are provided in the online version of this paper and include the following:

- KEY RESOURCES TABLE
- RESOURCE AVAILABILITY
  - Lead contact
  - Materials availability
  - Data and code availability
- EXPERIMENTAL MODEL AND STUDY PARTICIPANT DETAILS
- METHOD DETAILS
  - Selection of RNA modification regulators and genetic variation analyses
  - Supervised cluster analysis incorporating survival information weights
  - Assessment of tumor immune infiltration
  - RNA expression-based Assessment of stemness index (mRNAsi)
  - Analysis of transcriptional regulatory networks and chromatin-regulated activity between three subtypes
  - RNA modification-related signature construction and survival analysis
- GENE SET ENRICHMENT ANALYSIS (GSEA)
  - Chemotherapy and immunotherapy response with RNA modification-related signature
  - Cluster analysis of single-cell RNA-sequencing data and pseudotime analysis
- QUANTIFICATION AND STATISTICAL ANALYSIS
  - Additional resources

SUPPLEMENTAL INFORMATION

Supplemental information can be found online at https://doi.org/10.1016/j.isci.2024.108897.

ACKNOWLEDGMENTS

This work was supported by the following grants: National Key R&D Program of China (2021YFC2500400) to K.C; National Natural Science Foundation of China (82073028, 82372588) to B.L; National Natural Science Foundation of China (82172894) to K.C; The 14th five-year Special Project of Cancer Prevention and Treatment for the Youth Talents of Tianjin Cancer Institute and Hospital (YQ-04) to B.L; Beijing-Tianjin-Hebei

Basic Research Cooperation Special Project (grant 20JCZXJC00090) to K.C; Tianjin Key Medical Discipline (Specialty) Construction Project (TJYXZDXK-009A) to K.C. This work was supported by Cancer Biobank of Tianjin Medical University Cancer Institute and Hospital; National Human Genetic Resources Sharing Service Platform (2005DKA21300). The graphical abstract was created with BioRender.com (https://www.biorender.com/).

AUTHOR CONTRIBUTIONS

All authors have read and agreed to the published version of the manuscript. Conceptualization: X.H. and B.L.; methodology: W.X.; software: X.H.; validation: X.Z. and L.J.; formal analysis: W.X.; investigation: X.Z. and W.X.; resources: HL., W.W., and L.L.; data curation: L.J., Y.Y., and J.M.; writing - original draft: X.Z.; writing - review and editing: X.Z., L.J., and B.L.; visualization: X.Z.; supervision: B.L.; project administration: K.C.; funding acquisition: B.L. and K.C.

DECLARATION OF INTERESTS

The authors declare no competing interests.

Received: July 28, 2023
Revised: October 28, 2023
Accepted: January 9, 2024
Published: January 12, 2024

REFERENCES

1. Thrift, A.P., Wenker, T.N., and El-Serag, H.B. (2023). Global burden of gastric cancer: epidemiological trends, risk factors, screening and prevention. Nat. Rev. Clin. Oncol. *20*, 338–349.
2. Ishimoto, T., Miyake, K., Nandi, T., Yashiro, M., Onishi, N., Huang, K.K., Lin, S.J., Kalpana, R., Tay, S.T., Suzuki, Y., et al. (2017). Activation of Transforming Growth Factor Beta 1 Signaling in Gastric Cancer-associated Fibroblasts Increases Their Motility, via Expression of Rhomboid 5 Homolog 2, and Ability to Induce Invasiveness of Gastric Cancer Cells. Gastroenterology *153*, 191–204.e16.
3. Digklia, A., and Wagner, A.D. (2016). Advanced gastric cancer: Current treatment landscape and future perspectives. World J. Gastroenterol. *22*, 2403–2414.
4. Bray, F., Ferlay, J., Soerjomataram, I., Siegel, R.L., Torre, L.A., and Jemal, A. (2018). Global cancer statistics 2018: GLOBOCAN estimates of incidence and mortality worldwide for 36 cancers in 185 countries. CA. Cancer J. Clin. *68*, 394–424.
5. Ferro, A., Peleteiro, B., Malvezzi, M., Bosetti, C., Bertuccio, P., Levi, F., Negri, E., La Vecchia, C., and Lunet, N. (2014). Worldwide trends in gastric cancer mortality (1980-2011), with predictions to 2015, and incidence by subtype. Eur. J. Cancer *50*, 1330–1344.
6. Kietrys, A.M., and Kool, E.T. (2016). Epigenetics: A new methyl mark on messengers. Nature *530*, 423–424.
7. Petrovchich, I., and Ford, J.M. (2016). Genetic predisposition to gastric cancer. Semin. Oncol. *43*, 554–559.
8. Li, X., Pasche, B., Zhang, W., and Chen, K. (2018). Association of MUC16 Mutation With Tumor Mutation Load and Outcomes in Patients With Gastric Cancer. JAMA Oncol. *4*, 1691–1698.
9. Chen, Z., Qi, M., Shen, B., Luo, G., Wu, Y., Li, J., Lu, Z., Zheng, Z., Dai, Q., and Wang, H. (2019). Transfer RNA demethylase ALKBH3 promotes cancer progression via induction of tRNA-derived small RNAs. Nucleic Acids Res. *47*, 2533–2545.
10. Wang, Q., Chen, C., Ding, Q., Zhao, Y., Wang, Z., Chen, J., Jiang, Z., Zhang, Y., Xu, G., Zhang, J., et al. (2020). METTL3-mediated m(6)A modification of HDGF mRNA promotes gastric cancer progression and has prognostic significance. Gut *69*, 1193–1205.
11. Dunin-Horkawicz, S., Czerwoniec, A., Gajda, M.J., Feder, M., Grosjean, H., and Bujnicki, J.M. (2006). MODOMICS: a database of RNA modification pathways. Nucleic Acids Res. *34*, D145–D149.
12. Delaunay, S., and Frye, M. (2019). RNA modifications regulating cell fate in cancer. Nat. Cell Biol. *21*, 552–559.
13. Roundtree, I.A., Luo, G.-Z., Zhang, Z., Wang, X., Zhou, T., Cui, Y., Sha, J., Huang, X., Guerrero, L., Xie, P., et al. (2017). YTHDC1 mediates nuclear export of N-methyladenosine methylated mRNAs. Elife *6*, e31311.
14. Sun, T., Wu, R., and Ming, L. (2019). The role of m6A RNA methylation in cancer. Biomed. Pharmacother. *112*, 108613.
15. Wang, T., Kong, S., Tao, M., and Ju, S. (2020). The potential role of RNA N6-methyladenosine in Cancer progression. Mol. Cancer *19*, 88.
16. Mandel, C.R., Bai, Y., and Tong, L. (2008). Protein factors in pre-mRNA 3'-end processing. Cell. Mol. Life Sci. *65*, 1099–1122.
17. Guhaniyogi, J., and Brewer, G. (2001). Regulation of mRNA stability in mammalian cells. Gene *265*, 11–23.
18. Zhang, Y., Liu, L., Qiu, Q., Zhou, Q., Ding, J., Lu, Y., and Liu, P. (2021). Alternative polyadenylation: methods, mechanism, function, and role in cancer. J. Exp. Clin. Cancer Res. *40*, 51.
19. Yuan, F., Hankey, W., Wagner, E.J., Li, W., and Wang, Q. (2021). Alternative polyadenylation of mRNA and its role in cancer. Genes Dis. *8*, 61–72.
20. Orsolic, I., Carrier, A., and Esteller, M. (2023). Genetic and epigenetic defects of the RNA modification machinery in cancer. Trends Genet. *39*, 74–88.
21. Hamma, T., and Ferré-D'Amaré, A.R. (2006). Pseudouridine synthases. Chem. Biol. *13*, 1125–1135.
22. Zhao, B.S., and He, C. (2015). Pseudouridine in a new era of RNA modifications. Cell Res. *25*, 153–154.
23. Karikó, K., Muramatsu, H., Welsh, F.A., Ludwig, J., Kato, H., Akira, S., and Weissman, D. (2008). Incorporation of pseudouridine into mRNA yields superior nonimmunogenic vector with increased translational capacity and biological stability. Mol. Ther. *16*, 1833–1840.
24. De Almeida, C., Scheer, H., Zuber, H., and Gagliardi, D. (2018). RNA Uridylation: A Key Posttranscriptional Modification Shaping the Coding and Noncoding Transcriptome, *9* (Wiley Interdiscip Rev RNA).
25. Lim, J., Ha, M., Chang, H., Kwon, S.C., Simanshu, D.K., Patel, D.J., and Kim, V.N. (2014). Uridylation by TUT4 and TUT7 marks mRNA for degradation. Cell *159*, 1365–1376.
26. Chan, T.H.M., Qamra, A., Tan, K.T., Guo, J., Yang, H., Qi, L., Lin, J.S., Ng, V.H.E., Song, Y., Hong, H., et al. (2016). ADAR-Mediated RNA Editing Predicts Progression and Prognosis of Gastric Cancer. Gastroenterology *151*, 637–650.e10.e610.
27. Okugawa, Y., Toiyama, Y., Shigeyasu, K., Yamamoto, A., Shigemori, T., Yin, C., Ichikawa, T., Yasuda, H., Fujikawa, H., Yoshiyama, S., et al. (2018). Enhanced AZIN1 RNA editing and overexpression of its regulatory enzyme ADAR1 are important prognostic biomarkers in gastric cancer. J. Transl. Med. *16*, 366.
28. Mao, D., Zhou, Z., Song, S., Li, D., He, Y., Wei, Z., and Zhang, C. (2021). Identification of Stemness Characteristics Associated With the Immune Microenvironment and Prognosis in Gastric Cancer. Front. Oncol. *11*, 626961.
29. Guo, S.H., Ma, L., and Chen, J. (2022). Identification of Prognostic Markers and Potential Therapeutic Targets in Gastric Adenocarcinoma by Machine Learning Based on mRNAsi Index. J. Oncol. *2022*, 8926127.

30. Guo, R., Chu, A., and Gong, Y. (2020). Identification of cancer stem cell-related biomarkers in intestinal-type and diffuse-type gastric cancer by stemness index and weighted correlation network analysis. J. Transl. Med. *18*, 418.
31. Shi, X., Liu, Y., Cheng, S., Hu, H., Zhang, J., Wei, M., Zhao, L., and Xin, S. (2021). Cancer Stemness Associated With Prognosis and the Efficacy of Immunotherapy in Adrenocortical Carcinoma. Front. Oncol. *11*, 651622.
32. Yi, L., Huang, P., Zou, X., Guo, L., Gu, Y., Wen, C., and Wu, G. (2020). Integrative stemness characteristics associated with prognosis and the immune microenvironment in esophageal cancer. Pharmacol. Res. *161*, 105144.
33. Qin, S., Mao, Y., Wang, H., Duan, Y., and Zhao, L. (2021). The interplay between m6A modification and non-coding RNA in cancer stemness modulation: mechanisms, signaling pathways, and clinical implications. Int. J. Biol. Sci. *17*, 2718–2736.
34. Clara, J.A., Monge, C., Yang, Y., and Takebe, N. (2020). Targeting signalling pathways and the immune microenvironment of cancer stem cells - a clinical update. Nat. Rev. Clin. Oncol. *17*, 204–232.
35. Zhang, C., Zhang, M., Ge, S., Huang, W., Lin, X., Gao, J., Gong, J., and Shen, L. (2019). Reduced m6A modification predicts malignant phenotypes and augmented Wnt/PI3K-Akt signaling in gastric cancer. Cancer Med. *8*, 4766–4781.
36. Pi, J., Wang, W., Ji, M., Wang, X., Wei, X., Jin, J., Liu, T., Qiang, J., Qi, Z., Li, F., et al. (2021). YTHDF1 Promotes Gastric Carcinogenesis by Controlling Translation of FZD7. Cancer Res. *81*, 2651–2665.
37. Becerril-Rico, J., Alvarado-Ortiz, E., Toledo-Guzmán, M.E., Pelayo, R., and Ortiz-Sánchez, E. (2021). The cross talk between gastric cancer stem cells and the immune microenvironment: a tumor-promoting factor. Stem Cell Res. Ther. *12*, 498.
38. Chen, Y., Sun, Z., Chen, W., Liu, C., Chai, R., Ding, J., Liu, W., Feng, X., Zhou, J., Shen, X., et al. (2021). The Immune Subtypes and Landscape of Gastric Cancer and to Predict Based on the Whole-Slide Images Using Deep Learning. Front. Immunol. *12*, 685992.
39. Tzelepis, K., Rausch, O., and Kouzarides, T. (2019). RNA-modifying enzymes and their function in a chromatin context. Nat. Struct. Mol. Biol. *26*, 858–862.
40. Hyder, U., and D'Orso, I. (2021). Nascent RNA: Friend or foe of the chromatin bound? Mol. Cell *81*, 2871–2872.
41. Liu, J., Dou, X., Chen, C., Chen, C., Liu, C., Xu, M.M., Zhao, S., Shen, B., Gao, Y., Han, D., and He, C. (2020). N (6)-methyladenosine of chromosome-associated regulatory RNA regulates chromatin state and transcription. Science *367*, 580–586.
42. Xiao, R., Chen, J.Y., Liang, Z., Luo, D., Chen, G., Lu, Z.J., Chen, Y., Zhou, B., Li, H., Du, X., et al. (2019). Pervasive Chromatin-RNA Binding Protein Interactions Enable RNA-Based Regulation of Transcription. Cell *178*, 107–121.e18.
43. G Hendrickson, D., Kelley, D.R., Tenen, D., Bernstein, B., and Rinn, J.L. (2016). Widespread RNA binding by chromatin-associated proteins. Genome Biol. *17*, 28.
44. Kazlauskas, A. (2017). PDGFs and their receptors. Gene *614*, 1–7.
45. Mishra, Y.G., and Manavathi, B. (2021). Focal adhesion dynamics in cellular function and disease. Cell. Signal. *85*, 110046.
46. Lv, Y., Wang, X., Li, X., Xu, G., Bai, Y., Wu, J., Piao, Y., Shi, Y., Xiang, R., and Wang, L. (2020). Nucleotide de novo synthesis increases breast cancer stemness and metastasis via cGMP-PKG-MAPK signaling pathway. PLoS Biol. *18*, e3000872.
47. Zhang, S., Li, S., Guo, J.L., Li, N., Zhang, C.N., and Liu, J. (2021). Integrated Analysis of lncRNA-Associated ceRNA Network Identifies Two lncRNA Signatures as a Prognostic Biomarker in Gastric Cancer. Dis. Markers *2021*, 8886897.
48. Xiang, T., Yuan, C., Guo, X., Wang, H., Cai, Q., Xiang, Y., Luo, W., and Liu, G. (2021). The novel ZEB1-upregulated protein PRTG induced by Helicobacter pylori infection promotes gastric carcinogenesis through the cGMP/PKG signaling pathway. Cell Death Dis. *12*, 150.
49. Nagarsheth, N., Wicha, M.S., and Zou, W. (2017). Chemokines in the cancer microenvironment and their relevance in cancer immunotherapy. Nat. Rev. Immunol. *17*, 559–572.
50. Charoentong, P., Finotello, F., Angelova, M., Mayer, C., Efremova, M., Rieder, D., Hackl, H., and Trajanoski, Z. (2017). Pan-cancer Immunogenomic Analyses Reveal Genotype-Immunophenotype Relationships and Predictors of Response to Checkpoint Blockade. Cell Rep. *18*, 248–262.
51. Sheng, Y., Wei, J., Yu, F., Xu, H., Yu, C., Wu, Q., Liu, Y., Li, L., Cui, X.L., Gu, X., et al. (2021). A critical role of nuclear m6A reader YTHDC1 in leukemogenesis by regulating MCM complex-mediated DNA replication. Blood *138*, 2838–2852.
52. Kim, B.H., Jung, W.Y., Lee, H., Kang, Y., Jang, Y.J., Hong, S.W., Jeong, H.J., and Yoon, S.O. (2014). Lysyl-tRNA synthetase (KRS) expression in gastric carcinoma and tumor-associated inflammation. Ann. Surg Oncol. *21*, 2020–2027.
53. Nanthakumaran, S., Brown, I., Heys, S.D., and Schofield, A.C. (2009). Inhibition of gastric cancer cell growth by arginine: molecular mechanisms of action. Clin. Nutr. *28*, 65–70.
54. Delage, B., Fennell, D.A., Nicholson, L., McNeish, I., Lemoine, N.R., Crook, T., and Szlosarek, P.W. (2010). Arginine deprivation and argininosuccinate synthetase expression in the treatment of cancer. Int. J. Cancer *126*, 2762–2772.
55. Eniafe, J., and Jiang, S. (2021). The functional roles of TCA cycle metabolites in cancer. Oncogene *40*, 3351–3363.
56. Kim, Y.L., Lee, W., Chung, S.H., Yu, B.M., Lee, Y.C., and Hong, J. (2022). Metabolic alterations of short-chain fatty acids and TCA cycle intermediates in human plasma from patients with gastric cancer. Life Sci. *309*, 121010.
57. Wang, Y., Xie, S., and He, B. (2020). Mannose shows antitumour properties against lung cancer via inhibiting proliferation, promoting cisplatin-mediated apoptosis and reducing metastasis. Mol. Med. Rep. *22*, 2957–2965.
58. Mariathasan, S., Turley, S.J., Nickles, D., Castiglioni, A., Yuen, K., Wang, Y., Kadel, E.E., III, Koeppen, H., Astarita, J.L., Cubas, R., et al. (2018). TGFbeta attenuates tumour response to PD-L1 blockade by contributing to exclusion of T cells. Nature *554*, 544–548.
59. Huang, Y., Su, R., Sheng, Y., Dong, L., Dong, Z., Xu, H., Ni, T., Zhang, Z.S., Zhang, T., Li, C., et al. (2019). Small-Molecule Targeting of Oncogenic FTO Demethylase in Acute Myeloid Leukemia. Cancer Cell *35*, 677–691.e10.
60. Liu, Y., Liang, G., Xu, H., Dong, W., Dong, Z., Qiu, Z., Zhang, Z., Li, F., Huang, Y., Li, Y., et al. (2021). Tumors exploit FTO-mediated regulation of glycolytic metabolism to evade immune surveillance. Cell Metab. *33*, 1221–1233.e11.
61. Yu, H., Yang, X., Tang, J., Si, S., Zhou, Z., Lu, J., Han, J., Yuan, B., Wu, Q., Lu, Q., and Yang, H. (2021). ALKBH5 Inhibited Cell Proliferation and Sensitized Bladder Cancer Cells to Cisplatin by m6A-CK2alpha-Mediated Glycolysis. Mol. Ther. Nucleic Acids *23*, 27–41.
62. Taketo, K., Konno, M., Asai, A., Koseki, J., Toratani, M., Satoh, T., Doki, Y., Mori, M., Ishii, H., and Ogawa, K. (2018). The epitranscriptome m6A writer METTL3 promotes chemo- and radioresistance in pancreatic cancer cells. Int. J. Oncol. *52*, 621–629.
63. Nie, S., Zhang, L., Liu, J., Wan, Y., Jiang, Y., Yang, J., Sun, R., Ma, X., Sun, G., Meng, H., et al. (2021). ALKBH5-HOXA10 loop-mediated JAK2 m6A demethylation and cisplatin resistance in epithelial ovarian cancer. J. Exp. Clin. Cancer Res. *40*, 284.
64. Zhuang, H., Yu, B., Tao, D., Xu, X., Xu, Y., Wang, J., Jiao, Y., and Wang, L. (2023). The role of m6A methylation in therapy resistance in cancer. Mol. Cancer *22*, 91.
65. van de Donk, N.W.C.J., Usmani, S.Z., and Yong, K. (2021). CAR T-cell therapy for multiple myeloma: state of the art and prospects. Lancet. Haematol. *8*, e446–e461.
66. Mikkilineni, L., and Kochenderfer, J.N. (2021). CAR T cell therapies for patients with multiple myeloma. Nat. Rev. Clin. Oncol. *18*, 71–84.
67. Yu, B., Jiang, T., and Liu, D. (2020). BCMA-targeted immunotherapy for multiple myeloma. J. Hematol. Oncol. *13*, 125.
68. Song, Y., Zhang, Z., Zhang, B., and Zhang, W. (2022). CD8+ T cell-associated genes MS4A1 and TNFRSF17 are prognostic markers and inhibit the progression of colon cancer. Front. Oncol. *12*, 941208.
69. Qi, C., Gong, J., Li, J., Liu, D., Qin, Y., Ge, S., Zhang, M., Peng, Z., Zhou, J., Cao, Y., et al. (2022). Claudin18.2-specific CAR T cells in gastrointestinal cancers: phase 1 trial interim results. Nat. Med. *28*, 1189–1198.
70. Khan, A., Gamble, L.D., Upton, D.H., Ung, C., Yu, D.M.T., Ehteda, A., Pandher, R., Mayoh, C., Hébert, S., Jabado, N., et al. (2021). Dual targeting of polyamine synthesis and uptake in diffuse intrinsic pontine gliomas. Nat. Commun. *12*, 971.
71. Hogarty, M.D., Norris, M.D., Davis, K., Liu, X., Evageliou, N.F., Hayes, C.S., Pawel, B., Guo, R., Zhao, H., Sekyere, E., et al. (2008). ODC1 is a critical determinant of MYCN oncogenesis and a therapeutic target in neuroblastoma. Cancer Res. *68*, 9735–9745.
72. Rounbehler, R.J., Li, W., Hall, M.A., Yang, C., Fallahi, M., and Cleveland, J.L. (2009). Targeting ornithine decarboxylase impairs development of MYCN-amplified neuroblastoma. Cancer Res. *69*, 547–553.
73. Ye, Z., Zeng, Z., Shen, Y., Yang, Q., Chen, D., Chen, Z., and Shen, S. (2019). ODC1 promotes proliferation and mobility via the AKT/GSK3beta/beta-catenin pathway and modulation of acidotic microenvironment in

human hepatocellular carcinoma. OncoTargets Ther. *12*, 4081–4092.
74. Erichsen, L., Seifert, H.H., Schulz, W.A., Hoffmann, M.J., Niegisch, G., Araúzo-Bravo, M.J., Bendhack, M.L., Poyet, C., Hermanns, T., Beermann, A., et al. (2020). Basic Hallmarks of Urothelial Cancer Unleashed in Primary Uroepithelium by Interference with the Epigenetic Master Regulator ODC1. Sci. Rep. *10*, 3808.
75. Cho, L.Y., Yang, J.J., Ko, K.P., Ma, S.H., Shin, A., Choi, B.Y., Kim, H.J., Han, D.S., Song, K.S., Kim, Y.S., et al. (2015). Gene polymorphisms in the ornithine decarboxylase-polyamine pathway modify gastric cancer risk by interaction with isoflavone concentrations. Gastric Cancer *18*, 495–503.
76. Zhang, X., Hamblin, M.H., and Yin, K.J. (2017). The long noncoding RNA Malat1: Its physiological and pathophysiological functions. RNA Biol. *14*, 1705–1714.
77. Wang, Q., Chen, C., Xu, X., Shu, C., Cao, C., Wang, Z., Fu, Y., Xu, L., Xu, K., Xu, J., et al. (2022). APAF1-Binding Long Noncoding RNA Promotes Tumor Growth and Multidrug Resistance in Gastric Cancer by Blocking Apoptosome Assembly. Adv. Sci. *9*, e2201889.
78. Lee, J.H., Wang, R., Xiong, F., Krakowiak, J., Liao, Z., Nguyen, P.T., Moroz-Omori, E.V., Shao, J., Zhu, X., Bolt, M.J., et al. (2021). Enhancer RNA m6A methylation facilitates transcriptional condensate formation and gene activation. Mol. Cell *81*, 3368–3385.e9.
79. Zhao, Y., Wen, S., Li, H., Pan, C.W., Wei, Y., Huang, T., Li, Z., Yang, Y., Fan, S., and Zhang, Y. (2023). Enhancer RNA promotes resistance to radiotherapy in bone-metastatic prostate cancer by m(6)A modification. Theranostics *13*, 596–610.
80. Song, F., Yang, D., Liu, B., Guo, Y., Zheng, H., Li, L., Wang, T., Yu, J., Zhao, Y., Niu, R., et al. (2014). Integrated microRNA network analyses identify a poor-prognosis subtype of gastric cancer characterized by the miR-200 family. Clin. Cancer Res. *20*, 878–889.
81. Liu, B., Zhou, M., Li, X., Zhang, X., Wang, Q., Liu, L., Yang, M., Yang, D., Guo, Y., Zhang, Q., et al. (2021). Interrogation of gender disparity uncovers androgen receptor as the transcriptional activator for oncogenic miR-125b in gastric cancer. Cell Death Dis. *12*, 441.
82. Nishikura, K. (2016). A-to-I editing of coding and non-coding RNAs by ADARs. Nat. Rev. Mol. Cell Biol. *17*, 83–96.
83. Elkon, R., Ugalde, A.P., and Agami, R. (2013). Alternative cleavage and polyadenylation: extent, regulation and function. Nat. Rev. Genet. *14*, 496–506.
84. Chan, S.L., Huppertz, I., Yao, C., Weng, L., Moresco, J.J., Yates, J.R., 3rd, Ule, J., Manley, J.L., and Shi, Y. (2014). CPSF30 and Wdr33 directly bind to AAUAAA in mammalian mRNA 3′ processing. Genes Dev. *28*, 2370–2380.
85. Menezes, M.R., Balzeau, J., and Hagan, J.P. (2018). 3′ RNA Uridylation in Epitranscriptomics, Gene Regulation, and Disease. Front. Mol. Biosci. *5*, 61.
86. Arora, A., Olshen, A.B., Seshan, V.E., and Shen, R. (2020). Pan-cancer identification of clinically relevant genomic subtypes using outcome-weighted integrative clustering. Genome Med. *12*, 110.
87. Şenbabaoğlu, Y., Gejman, R.S., Winer, A.G., Liu, M., Van Allen, E.M., de Velasco, G., Miao, D., Ostrovnaya, I., Drill, E., Luna, A., et al. (2016). Tumor immune microenvironment characterization in clear cell renal cell carcinoma identifies prognostic and immunotherapeutically relevant messenger RNA signatures. Genome Biol. *17*, 231.
88. Lee, J., Kotliarova, S., Kotliarov, Y., Li, A., Su, Q., Donin, N.M., Pastorino, S., Purow, B.W., Christopher, N., Zhang, W., et al. (2006). Tumor stem cells derived from glioblastomas cultured in bFGF and EGF more closely mirror the phenotype and genotype of primary tumors than do serum-cultured cell lines. Cancer Cell *9*, 391–403.
89. Shibue, T., and Weinberg, R.A. (2017). EMT, CSCs, and drug resistance: the mechanistic link and clinical implications. Nat. Rev. Clin. Oncol. *14*, 611–629.
90. Batlle, E., and Clevers, H. (2017). Cancer stem cells revisited. Nat. Med. *23*, 1124–1134.
91. Malta, T.M., Sokolov, A., Gentles, A.J., Burzykowski, T., Poisson, L., Weinstein, J.N., Kamińska, B., Huelsken, J., Omberg, L., Gevaert, O., et al. (2018). Machine Learning Identifies Stemness Features Associated with Oncogenic Dedifferentiation. Cell *173*, 338–354.e15.
92. Miao, Y., Yang, H., Levorse, J., Yuan, S., Polak, L., Sribour, M., Singh, B., Rosenblum, M.D., and Fuchs, E. (2019). Adaptive Immune Resistance Emerges from Tumor-Initiating Stem Cells. Cell *177*, 1172–1186.e14.
93. Reddy, J., Fonseca, M.A.S., Corona, R.I., Nameki, R., Segato Dezem, F., Klein, I.A., Chang, H., Chaves-Moreira, D., Afeyan, L.K., Malta, T.M., et al. (2021). Predicting master transcription factors from pan-cancer expression data. Sci. Adv. *7*, eabf6123.
94. Audia, J.E., and Campbell, R.M. (2016). Histone Modifications and Cancer. Cold Spring Harb. Perspect. Biol. *8*, a019521.
95. Tan, M.H., Li, Q., Shanmugam, R., Piskol, R., Kohler, J., Young, A.N., Liu, K.I., Zhang, R., Ramaswami, G., Ariyoshi, K., et al. (2017). Dynamic landscape and regulation of RNA editing in mammals. Nature *550*, 249–254.
96. Shah, A., Mittleman, B.E., Gilad, Y., and Li, Y.I. (2021). Benchmarking sequencing methods and tools that facilitate the study of alternative polyadenylation. Genome Biol. *22*, 291.
97. Schwartz, S., Bernstein, D.A., Mumbach, M.R., Jovanovic, M., Herbst, R.H., León-Ricardo, B.X., Engreitz, J.M., Guttman, M., Satija, R., Lander, E.S., et al. (2014). Transcriptome-wide Mapping Reveals Widespread Dynamic-Regulated Pseudouridylation of ncRNA and mRNA. Cell *159*, 148–162.
98. Chang, H., Lim, J., Ha, M., and Kim, V.N. (2014). TAIL-seq: genome-wide determination of poly(A) tail length and 3′ end modifications. Mol. Cell *53*, 1044–1052.
99. Xuan, J.-J., Sun, W.-J., Lin, P.-H., Zhou, K.-R., Liu, S., Zheng, L.-L., Qu, L.-H., and Yang, J.-H. (2018). RMBase v2.0: deciphering the map of RNA modifications from epitranscriptome sequencing data. Nucleic Acids Res. *46*, D327–D334.
100. Geeleher, P., Cox, N., and Huang, R.S. (2014). pRRophetic: an R package for prediction of clinical chemotherapeutic response from tumor gene expression levels. PLoS One *9*, e107468.
101. Jeong, H.Y., Ham, I.H., Lee, S.H., Ryu, D., Son, S.Y., Han, S.U., Kim, T.M., and Hur, H. (2021). Spatially Distinct Reprogramming of the Tumor Microenvironment Based On Tumor Invasion in Diffuse-Type Gastric Cancers. Clin. Cancer Res. *27*, 6529–6542.

STAR★METHODS

KEY RESOURCES TABLE

REAGENT or RESOURCE	SOURCE	IDENTIFIER
Deposited data		
mRNA expression matrix	UCSC Xena	https://xenabrowser.net/datapages/
Somatic mutation information	UCSC Xena	https://xenabrowser.net/datapages/
TCGA-STAD RNA-seq	TCGA	https://portal.gdc.cancer.gov/
TCGA-STAD clinical data	UCSC Xena	https://xenabrowser.net/datapages/
GSE57303	GEO	https://www.ncbi.nlm.nih.gov/geo
GSE84437	GEO	https://www.ncbi.nlm.nih.gov/geo/
GSE13861	GEO	https://www.ncbi.nlm.nih.gov/geo/
GSE15459	GEO	https://www.ncbi.nlm.nih.gov/geo/
GSE26899	GEO	https://www.ncbi.nlm.nih.gov/geo/
GSE62254	GEO	https://www.ncbi.nlm.nih.gov/geo/
GSE34942	GEO	https://www.ncbi.nlm.nih.gov/geo/
GSE26901	GEO	https://www.ncbi.nlm.nih.gov/geo/
Tianjin (90 GC samples)	Tianjin Medical University Cancer Institute and Hospital	Song et al.[80]; Liu et al.[81]
TJ_206	Tianjin Medical University Cancer Institute and Hospital	N/A
Specific modification targets	RMBase v2.0	http://rna.sysu.edu.cn/rmbase/
Signaling pathways	Molecular Signaling Database (MSigDB)	https://www.gsea-msigdb.org/gsea/msigdb
Signaling pathways	Kyoto Encyclopedia of Genes and Genomes (KEGG)	https://www.genome.jp/kegg/
Signaling pathways	Gene Ontology (GO)	https://www.geneontology.org/
IMvigor210 cohort clinical information and gene expression data	IMvigor210 dataset	http://research-pub.gene.com/IMvigor210CoreBiologies Mariathasan et al.[58]
GSE167297 (ScRNA-seq dataset)	GEO	https://www.ncbi.nlm.nih.gov/geo/
Known cell marker genes	CellMarker database	https://ngdc.cncb.ac.cn/databasecommons/database/id/6110
Software and algorithms		
R (3.6.1)	R Core Team	https://www.r-project.org/
R (4.1.2)	R Core Team	https://www.r-project.org/
SurvClust algorithm	'survClust' R package	https://github.com/arorarshi/survClust
ssGSEA	'GSVA' R package	http://www.bioconductor.org
Single-cell RNA-sequencing analysis	'Seurat' R package	https://satijalab.org/seurat/
Chemotherapeutic response prediction	'pRRophetic' R package	http://genemed.uchicago.edu/~pgeeleher/pRRophetic

RESOURCE AVAILABILITY

Lead contact

Further information and requests for resources and materials should be directed to and will be fulfilled by the lead contact, Ben Liu (benliu100@tmu.edu.cn).

Materials availability

This study did not generate new unique reagents.

Data and code availability

- Publicly available datasets were analyzed in this study. The data involved in this article could be downloaded directly in TCGA-STAD (https://portal.gdc.cancer.gov/) and GEO (https://www.ncbi.nlm.nih.gov/geo/) datasets (GSE57303, GSE84437, GSE13861, GSE15459, GSE26899, GSE62254, GSE34942, GSE26901, GSE167297). Accession numbers are listed in the key resources table.
- Any additional information required to reanalyze the data reported in this paper is available from the lead contact upon request.
- No custom codes were used in the study.

EXPERIMENTAL MODEL AND STUDY PARTICIPANT DETAILS

This study used public data from the Cancer Genome Atlas (TCGA, https://portal.gdc.cancer.gov/), Gene Expression Omnibus (GEO, https://www.ncbi.nlm.nih.gov/geo/), and UCSC Xena databases. The platform information and sample numbers for each dataset are detailed in Table S6. The mRNA expression matrix, mutation information, and clinical information of the TCGA-STAD (The Cancer Genome Atlas-Stomach Adenocarcinoma, n = 350) were downloaded from UCSC Xena (https://xenabrowser.net/datapages/). The demographic characteristics were reported in Table S7. The values of their expression matrices were FPKM values from high-throughput sequencing, converted from FPKM to TPM to make them more comparable, and finally normalized for expression values using log2 (TPM+1). The gene names were annotated using the annotation file gencode.v22, and the maximum value was taken for genes with multiple FPKM values.

Expression matrices and clinical information were downloaded from the GEO database for eight GC cohorts, namely GSE57303 (n = 70), GSE84437 (n = 433), GSE13861 (n = 64), GSE15459 (n = 192), GSE26899 (n = 93), GSE62254 (n = 283), GSE34942 (n = 56), GSE26901 (n = 109). The demographic characteristics were reported in Table S8. Gene names were annotated using the platform file for each dataset, and for genes with multiple expression values, the maximum value was taken. Batch effects were removed using the COMBAT function of the R package 'sva'.

The two independent in-house cohorts of Tianjin (N = 90),[80,81] and TJ_206 (N = 206) were obtained from the Tumor Tissue Bank of the Tianjin Cancer Hospital. The demographic characteristics were reported in Table S9. The RNA sequencing of all samples from the TJ_206 cohort was performed using Illumina NovaSeq 6000. The samples were all from gastric cancer cases with precise histological and pathological diagnoses. All cases in this study were anonymous and processed according to legal requirements and medical standards, approved by the Ethics Committee of the Tianjin Medical University Cancer Hospital and Institute, and all informed consent was obtained from all patients.

METHOD DETAILS

Selection of RNA modification regulators and genetic variation analyses

Fifty-six genes associated with the regulation of five RNA modifications were obtained from the literature, including m6A (ALKBH5, ALKBH5, CBLL1, ELAVL1, FMR1, FTO, HNRNPA2B1, HNRNPC, IGF2BP1, IGF2BP2, IGF2BP3, KIAA1429, LRPPRC, METTL14, METTL16, METTL3, RBM15, RBM15B, WTAP, YTHDC1, YTHDC2, YTHDF1, YTHDF2, YTHDF3, ZC3H13), A-to-I editing (ADAR, ADARB1, ADARB2),[82] APA (CFI, CLP1, CPSF1, CPSF2, CPSF3, CPSF4, CSTF1, CSTF2, CSTF3, FIP1L1, NUDT21, PABPN1, PCF11, WDR33),[83,84] pseudouridine (DKC1, PUS1, PUS3, PUS4, PUS7, PUS7L, PUSL1, RPUSD1, RPUSD2, RPUSD3, RPUSD4, TRUB2),[21] and uridylation (TUT1, TUT4, TUT7).[85] Mutation waterfalls for these 56 genes in the TCGA-STAD cohort were mapped using the R package 'maftools', and CNV variation in these regulators on chromosomes was mapped using the R package 'OmicCircos'.

Supervised cluster analysis incorporating survival information weights

Patients were clustered in a supervised manner using survClust algorithm,[86] based on the mRNA expression of 56 RNA modification-related genes, incorporating weights for survival information. The appropriate number of clusters was selected using a log rank test statistic and a standardized intra-cluster sum of squares calculated by cross-validation. The optimal choice of clusters is made when the log rank test statistic reaches a maximum value and the standardized intra-cluster sum of squares curve decreases to an inflection point. It has been verified that clustering is optimal when the number of clusters is three. TCGA-STAD, GSE13861, GSE15459, GSE26899, GSE62254, Tianjin, GSE34942, and GSE26901 were integrated as the training set; GSE57307 and GSE84437 were integrated as the validation set.

Assessment of tumor immune infiltration

The tumor immune microenvironment, including immune score, stromal score, and tumor purity, was assessed in individual samples using the R package 'estimate'. 28 immune cells were derived from previous studies and contained both innate immune cells, such as eosinophils, mast cells, and macrophages, and adaptive immune cells, such as $CD4^+$ T cells and γδ T cells.[50,87] The single sample gene sets enrichment analysis (ssGSEA) algorithm of the R package 'GSVA' was used to assess the abundance of 28 immune cell infiltrations in individual samples. In addition, we also assessed immune cell infiltration abundance by other algorithms, including CIBERSORT, MCPCounter, and TIMER, implemented through the CIBERSORT function, MCPcounter, and the R packages 'IOBR', respectively.

RNA expression-based Assessment of stemness index (mRNAsi)

Stemness reflects the potential for cell self-renewal and differentiation from cells of origin, and tumor-initiating stem cells (tSCs) have a strong capacity for self-renewal and differentiation.[88] Typically, undifferentiated primary tumors are more malignant and proliferative, leading to

disease progression and poor prognosis, and often exhibit drug resistance.[89,90] Therefore, Tathiane et al. used information on stem cell classes and their differentiated ectodermal, mesodermal, and endodermal progenitors, as well as transcriptional data, to construct a model using a one-class logistic regression (OCLR) machine-learning algorithm to derive mRNAsi and assess the degree of stemness of tumor cells.[91,92] The mRNAsi reflects the gene expression profile of stem cells in tumor samples. The model based on the training set was then applied to the nine test datasets used in this study to calculate the mRNAsi for each sample. The mRNAsi was normalized to between 0 and 1 to assess the stemness characteristics of the samples.

Analysis of transcriptional regulatory networks and chromatin-regulated activity between three subtypes

A transcriptional regulatory network consisting of 9 gastric cancer-specific transcription factors as well as 56 RNA regulatory enzymes[93] and a network of 71 chromatin-regulated associated factors was constructed using R package RTN.[94] Reciprocal information analysis and Spearman rank order correlation inferred possible associations between regulatory factors and all potential targets from transcriptome expression profiles and eliminated associations with FDR >0.00001 using alignment analysis. Unstable associations were then eliminated by 1000 re-samplings with a consistent bootstrap rate of >95%. Ultimately, bilateral GSEA was used to assess individual regulator activity.

RNA modification-related signature construction and survival analysis

The above RNA modification targets were collected from previous studies validated by sequencing and predicted by RMBase (http://rna.sysu.edu.cn/rmbase), plus 56 RNA modification enzymes. After removing duplicates and intersecting with the existing dataset, 2943 targeted DEGs were obtained for the further step of signature construction.[95–99] Next, we merged cluster2 and cluster3 and performed differential expression analysis with cluster1, resulting in 315 differentially expressed genes ($p < 0.05$ and $|\log \text{fold change}| > 0.5$). We conducted univariate Cox regression analysis on the training dataset GSE84437 of these 315 DEGs (Table S10), yielding 94 genes with prognostic differences. Next, Stepwise Regression Analysis obtained 24 DEGs. The signature was constructed via Random Survival Forest. TCGA-STAD, GSE13861, GSE15459, GSE26899, GSE62254, GSE57307, GSE34942, GSE26901, Tianjin and TJ_206 were used separately as independent validation datasets.

Based on the cut-off values, the patients were assigned to a high- and low-risk group. The Kaplan-Meier method was used to assess the efficiency of overall survival (OS) and recurrence-free survival (RFS) in high- and low-risk patients. The log rank test was used to assess statistical significance at $p < 0.05$.

GENE SET ENRICHMENT ANALYSIS (GSEA)

To explore differences in biological function between subtypes, we downloaded signaling pathways from the Molecular Signaling Database (MSigDB) and assessed changes in pathways and biological process activities between subtypes by Gene Set Enrichment Analysis (GSEA), which was implemented by the R package 'GSVA'. The Kyoto Encyclopedia of Genes and Genomes (KEGG) and Gene Ontology (GO) results are exhibited by a GSEA plot. FDR <0.05 was considered statistically significant.

Chemotherapy and immunotherapy response with RNA modification-related signature

Chemotherapeutic response in GC patients was predicted using the R package 'pRRophetic'.[100] Immunotherapy response was validated by an immunotherapeutic dataset of advanced urothelial cancer (IMvigor210 cohort).[58] Clinical information and gene expression data were extracted from the IMvigor210 dataset (http://research-pub.gene.com/IMvigor210CoreBiologies).

Cluster analysis of single-cell RNA-sequencing data and pseudotime analysis

ScRNA-seq dataset (GSE167297) from 14 GC samples from GEO[101] were preprocessed and subsequently analyzed by the 'Seurat' R package. Uniform Manifold Approximation and Projection (UMAP) was applied to dimensionality reduction single-cell data and visualized the cell atlas. To filter out low-quality cells and genes, we selected cells with transcripts >300 per cell, expressed in more than three cells per transcript, the percentage of mitochondrial ratios <10%, and ribosome ratios >3% for further analyses. Monocle 3 describes how cells transition between transcriptome states. Major cell lineages were defined using known cell marker genes derived from the CellMarker database (https://ngdc.cncb.ac.cn/databasecommons/database/id/6110) or the literature.

QUANTIFICATION AND STATISTICAL ANALYSIS

R 3.6.1 and R 4.1.2 were used for statistical analyses (https://www.r-project.org/). Supervised clustering of samples was performed using the R package 'survClust'. The Kaplan-Meier method in the R package 'survminer' was used to plot survival curves between subtypes. The log rank test was used to assess whether differences in survival between subtypes were statistically significant. p-value correction for multiple testing was performed using the Benjamini-Hochberg method. Univariate analysis of differences in the distribution of continuous variables was performed using the Wilcoxon test. Multi-factor Cox analysis was used to correct for the effect of confounding factors such as age, gender, and stage on prognosis. All tests were two-sided. p-values less than 0.05 were considered statistically significant differences unless specified.

Additional resources

This study did not generate additional data.